Journal of Mining and Geology Vol. 57(2) 2021. pp. 407 - 426 0022-2763

Upper Lithospheric Structure of the Middle Benue Trough, Nigeria, Derived from Analysis of Satellite Gravity Data

Anudu, G.K.[1,2] and Obrike, S.E.[1,2]
[1]Department of Geology and Mining, Nasarawa State University, PMB 1022, Keffi, Nigeria.
[2]Institute of Geosciences and Earth Resources, Nasarawa State University, PMB 1022, Nigeria.
Corresponding E-mail: zobrike@gmail.com

Abstract
The middle Benue Trough is the central segment of the Benue Trough, an elongate northeast orientated intracratonic rift basin in Nigeria. This study provides new information on the morphology/geometry of the upper lithospheric structures (Moho, crystalline crust thickness and crustal stretching factor) and tectonics in the middle Benue Trough and adjacent basement complex regions by analysis and three-dimensional (3D) inverse modelling of satellite Bouguer gravity anomaly data. Results from 3D inverse modelling reveal Moho depths varying from c. 24 ± 2 to 32 ± 3 km and crystalline crustal thickness values ranging between c. 20 ± 2 and 32 ± 3 km. Shallow Moho and thin crust occur beneath the Trough axial region, whereas deep Moho and thick crust underlay the basement complex regions and the Trough northwestern region. It also shows the presence of a prominent northeast-southwest (NE-SW) orientated, shallow Moho structures (c. 24 ± 2 to 27 ± 3 km deep) and thin crust (c. 20 ± 2 to 26 ± 3 km thick) within the Trough axial region. Comparisons of Moho depths with topography and Bouguer gravity anomaly values using profiles highlight that the observed broad, longer-wavelength near-positive Bouguer gravity anomalies over the Trough axial region are strongly associated with elevated (shallow) Moho and isostatic effect of lower topography. Crustal stretching factor (β) values obtained across the area range between c. 1.03 and 1.59 with moderately high values (c. 1.25 – 1.59) occurring in the Trough axial region. The tectonic implication of the results is that the crust/lithosphere beneath middle Benue Trough has been strongly affected/modified by intense regional, extensional and/or wrench (strike-slip) tectonics associated with past rifting events.

Keywords: *Benue Trough, Bouguer gravity, Moho, crust thickness, stretching factor, Nigeria.*

Highlights

- The 3D inversion applied to the satellite BA grid data reveals remarkable lateral variations in Moho depths and/or Moho morphology beneath the study area
- The imaged Moho and crystalline crust structures beneath the Trough axial region exhibit a major NE-SW orientation which is strikingly similar to the orientation of the Benue Trough, structures and regional Bouguer gravity anomalies.
- The study reveals that the shallow faulted crustal basements, shallow Moho and thin crystalline crust that characterised the Trough axial region were mainly formed through (regional) extensional tectonics which affected the underlying crust/lithosphere during rifting events in the Early to Late Cretaceous.

Introduction

The middle Benue Trough is the central segment of the Nigerian Benue Trough, an elongate large (c.1000 km long, c.120 -150 km wide) northeast trending intracratonic rift structure that formed by rifting of the Precambrian crustal basement of a Pan-African mobile belt in the Late Jurassic to Early Cretaceous and its formation is associated with the Equatorial and South Atlantic opening (e.g. Burke and Whiteman, 1973; Burke and Dewey, 1974; Olade, 1975; Wright, 1976, 1981; Whiteman, 1982; Fairhead and Binks, 1991; Guiraud and Maurin, 1991, 1992, 1993; Janssen et. al., 1995; Guiraud et al., 2005 Obaje, 2009; Nwajide, 2013, Anudu, 2017; Anudu et al., 2020 and reference therein; cf. Figure 1). Imaging the morphology/geometry and understanding the characters of the underlying upper lithospheric structures (e.g. Moho, crystalline crust thickness) beneath intracratonic rift basins (such as the Benue Trough) as well as crystalline basement complexes in different parts of the world are typically obtained through the analysis/modelling of seismic refraction, teleseismic and/or gravity datasets (e.g. Stephenson et al., 1994, 2017; Fichler et al., 2011; Bocin et al., 2013; Jordan et al., 2013; Blakely et al., 2014; Damiani et al., 2014; Curto et al., 2015; Fairhead, 2015; Anudu, 2017). Also in areas of the world where seismic refraction or teleseismic datasets are lacking, sparse or irregular, the analysis/modelling of any available medium- to high-resolution gravity data remains a robust approach to image the morphology/geometry of upper lithospheric structures and their characters (e.g. Fichler et al., 2011; Bocin et al., 2013; Jordan et al., 2013; Blakely et al., 2014; Curto et al., 2015; Anudu, 2017; Stephenson et al., 2017; Kusznir et al., 2018).

In the Benue Trough and adjoining basement complexes, several geophysical studies previously conducted at different points, locations and/or along different profiles have reported the presence of an elevated Moho (c. 22 – 27 km deep) and thinned crust beneath the Trough, as well as Moho depths and/or crustal thickness estimates of c. 29 – 35 km beneath the basement complexes (e.g. Adighije, 1981; Stuart et al., 1985; Fairhead and Okereke, 1987, 1988, 1990; Okereke, 1988; Tokam et al., 2010; Gallacher and Bastow, 2012; Akpan et al., 2016). These aforementioned previous works on the upper lithospheric structures across the Benue Trough and adjacent basement complexes have been based on gravity data (Adighije, 1981; Fairhead and Okereke, 1987, 1988, 1990; Okereke, 1988) and limited available seismic refraction (Stuart et al., 1985) as well as teleseismic (Tokam et al., 2010; Gallacher and Bastow, 2012; Akpan et al., 2016) data. These studies have focused on its upper (northeastern) segment as well as lower (southwestern) segment where teleseismic data and/or seismic refraction data are available (Figure 1). In contrast, teleseismic data and/or seismic refraction data are completely lacking in the middle Benue Trough segment and the few studies that have been done on its upper lithospheric structures are based from the analysis of ground gravity data along one or two profiles (Adighije, 1981; Fairhead and Okereke, 1987; Okereke, 1988). Accordingly, these few previous studies were unable to determine and/or map in detail the morphology/geometry and lateral extent of the upper lithospheric structures (e.g. Moho, crystalline crust thickness) across the middle Benue Trough and adjoining basement complexes, due to the limitations of ground gravity data as well as gravity profile (2D) forward modelling method. Hence, the detailed morphology/geometry and lateral extents of the underlying upper lithospheric structures across the area are still relatively poorly known.

Therefore, this present study is aimed at providing new and more detailed insight on the morphology/geometry and lateral extents of the underlying upper lithospheric structures (e.g. Moho, crystalline crust thickness) in the middle Benue Trough and adjoining regions by three-dimensional (3D) inverse modelling of the (moderate-resolution) satellite Bouguer gravity anomaly data. Specific objectives are interpreting the Bouguer gravity anomalies, determining Moho depths/morphology, estimating crystalline crustal thickness and crustal stretching factor values across the area, as well as their variations and tectonic/geodynamic implication.

Geology and Tectonics

The study area is flanked in the north and southeast by the Northern Nigerian Basement Complex and the Eastern Nigerian Basement Complex, respectively (Figure 2a). It is underlain by four distinct rock types: basement complex rocks, Younger Granite complexes, sedimentary rocks and magmatic rocks (e.g. Offodile, 1976, 1989; Ajayi and Ajakaiye, 1981, 1986; Benkhelil, 1989; Obaje, 2009; NGSA, 2009; Nwajide, 2013; Anudu et al., 2014, Anudu, 2017; Figure 2a). The basement complex rocks (Precambrian-Early Palaeozoic/Pan-African in age) consist mainly of migmatites, gneisses, granite-gneisses, granites and schists (e.g. Ajibade et al., 1989; McCurry, 1989; Rahaman, 1989; Dada, 1999). These rocks have been affected by the well-known Pan-African orogenic events (600 ± 200 Ma), as well as intruded by dolerite dykes and the Jurassic Younger Granites complexes (composed mainly of microgranites, biotite granites and rhyolites) particularly in the Northern Nigerian Basement Complex region (e.g. Bowden and Kinnaird, 1984; Badejoko, 1986; Bowden et al., 1987; Obaje, 2009). Also sedimentary rocks (Cretaceous in age) are found only within the Trough region and composed of the following: Asu River Group, Awe Formation, Keana Formation, Ezeaku Formation, Markudi Formation, Awgu Formation and the Lafia Formation (e.g. Offodile, 1976, 1989; Offodile and Reyment, 1977; Benkhelil, 1986, 1989; Obaje and Hamza, 2000; Obaje, 2009; Nwajide, 2013; Anudu et al., 2014, Anudu, 2017; Figure 2a). Sedimentary rocks older than the Late Santonian have been affected by the Late Santonian (ca. 86 Ma) compressional event which resulted in the formation of numerous NE-SW trending folds, faults and uplifts observed across the Trough (e.g. Benkhelil, 1989; Nwajide, 2013). Mafic to intermediate magmatic rocks (Early Cretaceous-Late Palaeogene in age) intruded the sedimentary rocks (Figure 2a) and they consist mainly of basalts, dolerites, diorites, gabbros phonolites, syenites and trachytes (Benkhelil, 1987; Benkhelil, 1989; Nwajide, 2013). These magmatic rocks occur mainly around southwest of Gboko, Awe, Arufu, Igbor, Kegh and Makurdi located within the axial region of the Trough (Offodile, 1976, 1989; Adighije, 1981; Umeji, 1985, 2000; Benkhelil et al., 1988; Maluski et al., 1995; Obiora, 2002; Nwajide, 2013; Anudu et al., 2014, Anudu, 2017; cf. Figure 2). Also, recent detailed magnetic studies conducted by Anudu et al. (2014) and Anudu (2017) identified and mapped numerous (mafic to intermediate) magmatic rocks (volcanic, sub-volcanic and intrusive) around Awe, Arufu, Igbor, Kegh and Makurdi as well as across the southwest of Gboko area situated within the Trough axial region; their published magmatic rock distribution map is presented in Figure 2b. Furthermore, several field geological studies revealed that numerous economic mineral deposits (e.g. barites, lead-zinc sulphides), salts, coals and warm to hot (thermal)

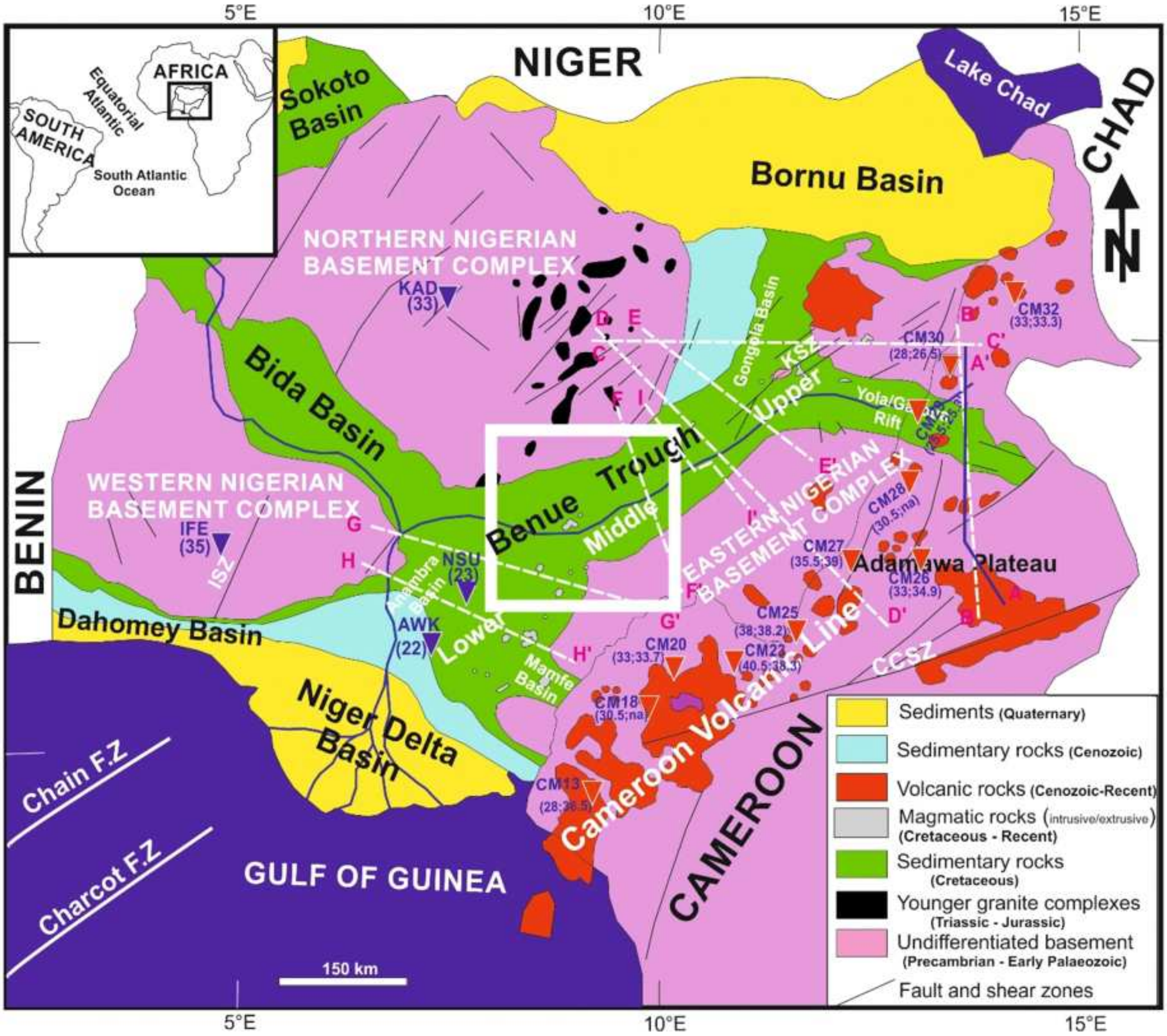

Fig. 1: Simplified regional geological map of Nigeria and surroundings showing the Benue Trough and adjoining basement complexes. The surface geology is largely modified and/or redrawn from Woakes et al. (1987), Obaje (2009) and International Geological Map of Africa 1:5,000,000 (Third Edition 1985 – 1990) with additional information from Wright et al. (1985), Benkhelil et al. (1988) and Anudu (2017). Insert is a map of Africa and South America showing the location of Nigeria and its surrounding regions in Africa. The Benue Trough subdivisions: lower, middle and upper are also shown. Location of the study area (middle Benue Trough region) is outlined with a white box (and this area is shown in Figure 2a). Blue triangles indicate the teleseismic stations of Akpan et al. (2016) with their names and Moho depth estimates (in bracket); red triangles mark the teleseismic stations of Tokam et al. (2010) and Gallacher and Bastow (2012) with their names and Moho depth estimates (in bracket). Profile AA^1 (thick blue line) indicates the seismic refraction profile (Stuart et al., 1985); profiles BB^1 – DD^1 (dashed white lines) mark the gravity profiles of Fairhead and Okereke (1987, 1988, 1990) and Okereke (1988); profiles EE^1 – HH^1 (dashed white lines) indicate gravity profiles of Adighije (1981a); profile II^1 (dashed white line) indicates gravity profile of Cratchley *et al*. (1984). The Yola/Garoua Rift, Cameroon Volcanic Line and Central Cameroon Shear Zone (CCSZ) are also shown.

springs/brines are found at different locations within the axial region of the Trough (e.g. Offodile, 1980; Whiteman, 1982; Wright et al., 1985; Akande et al., 1988, 1989; Nwajide, 2013; Anudu, 2017). In addition, several published field geological works (e.g. Rahaman et al., 1984; Maurin et al., 1986; Ajibade et al., 1989; Ajibade and Wright, 1989; Benkhelil et al., 1988; 1989; Guiraud et al., 1989; Guiraud, 1990; Aina et al., 1996; Rahaman, 1989; Obaje, 2009) and magnetic studies (e.g. Benkhelil et al., 1988; 1989; Aina et al., 1996; Anudu et al., 2012; 2014, 2020; Anudu, 2017) reported the presence of numerous geological structures (mainly faults/fracture systems and shear zones) exhibiting NE-SW, NNE-SSW, NW-SE, ENE-WSW and ESE-WNW major trends with minor N-S and E-W trends across the Trough and adjoining basement complexes (Figure 2). Most of these field observed major faults/fracture systems and shear zones are (mostly) Pan-African in age (e.g. Rahaman et al., 1984; Maurin et al., 1986; Ajibade et al., 1989; Ajibade and Wright, 1989; Benkhelil et al., 1989; Guiraud et al., 1989; Rahaman, 1989; Obaje, 2009).

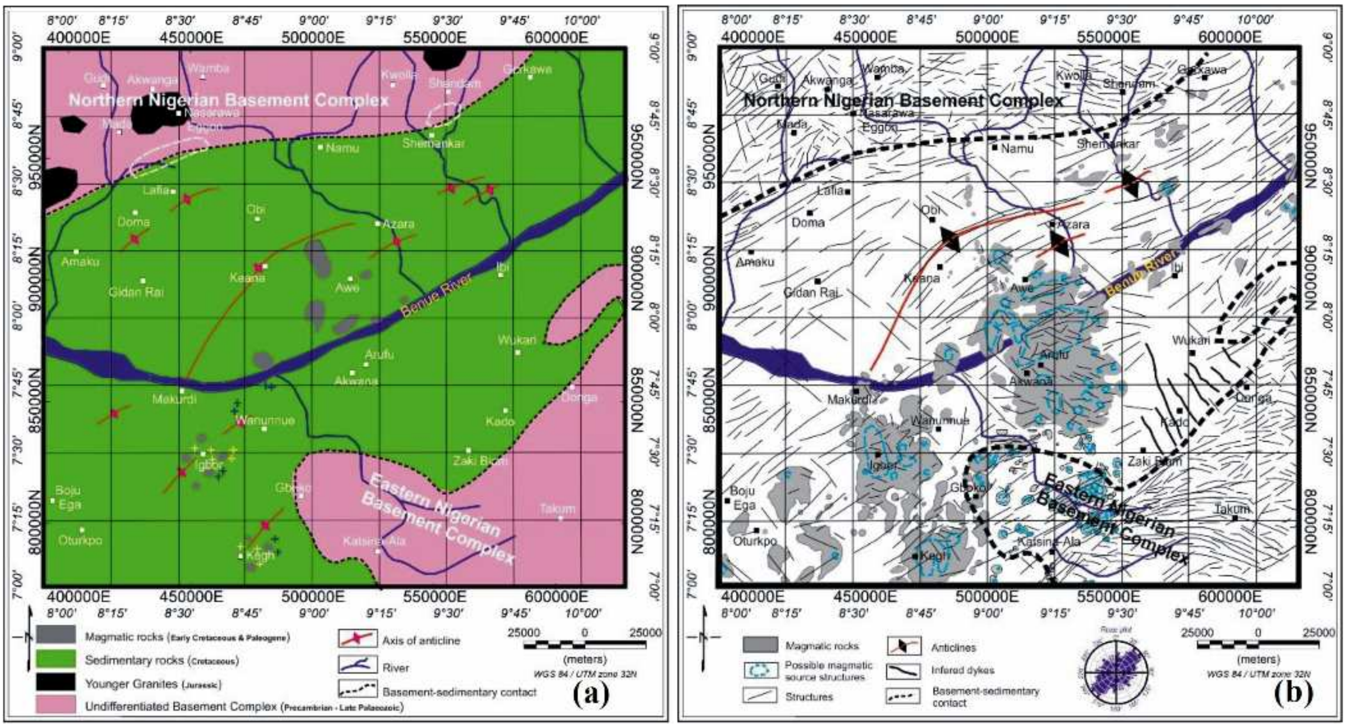

Fig. 2: (a) Geological map of the study area (extracted from Figure 1 with additional information added from Offodile, 1976; Ajayi and Ajakaiye, 1981, 1986; NGSA, 2009; Nwajide, 2013); locations of outcropping dolerites, diorites and gabbros recently identified/mapped by Nwajide (2013) have been indicated with a pink, blue, and yellow cross, respectively. **(b)** Magmatic rock and structural distribution map of the area (after Anudu et al., 2014; Anudu, 2017); it was delineated and mapped from detailed magnetic studies by Anudu *et al.* (2014) and Anudu (2017). Rose plot of the trends of structures derived from detailed magnetic studies (Anudu et al., 2014, 2020; Anudu, 2017) across the area depicts NE-SW, NNE-SSW, ENE-WSW/E-W and NW-SE/NNW-SSE trends with the NE-SW as dominant structural trend. Note that the dashed black lines outline the basement-sedimentary contact in both figures and other subsequent figures in this paper.

Datasets and Methods

Datasets

The datasets used in this study consist of the digital airborne topography data, basement depth data and satellite Bouguer gravity data. The airborne topography (surface digital elevation) data are part of the recent global 3-arc-second (~ 90 m resolution) topography grid (SRTM 90m) database of the Earth acquired by the Shuttle Radar Topography Mission (SRTM) (Jarvis et al., 2008; http://www.cgiar-csi.org/data/srtm-90m-digital-elevation-database-v4-1). This data grid was extracted/downloaded from the CGIAR-CSI SRTM data centre server (http://srtm.csi.cgiar.org/) and re-gridded/re-sampled at 1.5 km grid interval employing the minimum curvature gridding method (cf. Billings and Richards, 2000; Nabighian et al., 2005; Anudu, 2017) to generate the relief topography (surface elevation) map of the study area shown in Figure 3a.

The basement depth data used in this study is the same depth to basement (sediment thickness) grid data recently obtained by Anudu (2017) and Anudu et al. (2020). This basement depth data is the mean depth to basement (sediment thickness) result computed from the integration of numerous depth estimates obtained from the detailed analysis of preconditioned high-resolution aeromagnetic data using three grid-based semi-automated depth-estimation methods- total gradient (TG), horizontal gradient magnitude (HGM) and Source Parameter Imaging™ (SPI™) (cf. Anudu, 2017; Anudu et al., 2020). The aforementioned basement depth grid data has a grid size of 1.5 × 1.5 km and was re-gridded/re-sampled in the same way as the topography data, and the resulting basement depth map of the study area is presented in Figure 3b.

The satellite Bouguer gravity data used in this study is part of the moderate resolution World Gravity Map 2012 (WGM2012) satellite datasets obtained through the compilation of numerous regional terrestrial (ground), airborne and marine gravity surveys as well as satellite gravimetry of the Gravity Recovery and Climate Experiment (GRACE) mission (Bonvalot et al., 2012 and references therein). Important gravity data reductions/corrections applied to the data to derive the Bouguer gravity anomalies have been discussed in

Balmino et al. (2012) and references therein. The Bouguer gravity anomaly (BA) data grid was released for this study by the Bureau Gravimétrique International (BGI) France (http://bgi.omp.obs-mip.fr/) and re-sampled/re-gridded in the same way as the aforementioned topography and basement depth grid datasets. The resulting Bouguer gravity anomaly (BA) map of the study area is shown in Figure 3c.

Methods

Regional - Residual Bouguer Gravity Anomaly Separation

Bouguer gravity anomalies are characterised by a shorter-wavelength anomalies (known as residual Bouguer gravity anomaly; i.e. residual-BA) arising from shallower geological bodies, which are superimposed on a longer-wavelength gently varying anomalies (known as regional Bouguer gravity anomaly; i.e. regional-BA) associated with deeper (deep-seated) geological bodies and/or crustal structures (cf. Telford et al., 1990; Sheriff, 2002; Hinze et al., 2013; Fairhead, 2015). Thus, regional-residual Bouguer gravity anomaly separation is basically a process of separating the BA fields into its components (i.e. regional-BA and residual-BA) in order to get a better understanding of the subsurface geology and crustal structures (e.g. Telford et al., 1990; Sheriff, 2002; Hinze et al., 2013; Fairhead, 2015; Anudu, 2017). It is commonly carried out using different methods, namely: graphical, polynomial fitting, upward continuation, and wavelength filtering (e.g. Dobrin and Savit, 1988; Jacoby and Smilde, 2009; Nabighian et al., 2005; Hinze et al., 2013; Fairhead, 2015).

In this study, the wavelength filtering method (through the application of a Butterworth low-pass filter based on result derived from spectral analysis of the BA data grid) was used because it is a better method than the others since it can be used to identify the best separation point between the deeper and shallower sources (e.g. Nabighian et al., 2005; Hinze et al., 2013; Fairhead, 2015; Anudu, 2017). The result derived from spectral analysis of the BA data grid is shown in Figure 3d. Thus based on the spectral analysis result (Figure 3d), a Butterworth low-pass filter with a cut-off wavelength of 120000 m (120 km) (which corresponds to anomalies originating at an average depth of about 28000 m) was chosen and applied to the BA data grid to produce the required regional-BA map presented in Figure 4a. This map (Figure 4a) contains Bouguer gravity anomalies with wavelengths greater than 120 km, since the aforementioned filter applied has removed most anomalies with wavelengths shorter than 120 km. Subsequently, the residual-BA grid of the area (shown in Figure 4b) was derived by simply subtracting the regional-BA grid (Figure 4a) from the BA grid (Figure 3c); the resulting residual-BA grid/map (Figure 4b) contains Bouguer gravity anomalies with wavelengths shorter than 120 km.

Three-Dimensional (3D) Bouger Gravity Anomaly Data Inverse Modelling

This section involves a three-dimensional (3D) inverse modelling of the BA grid data to estimate the Moho morphology and depth information beneath the study area. It is important to state that the 3D inverse modelling of BA grid data also has been widely used for estimating the Moho depths and/or Moho morphology in different parts of the world, especially in areas with sparse/irregular or no seismic/teleseismic datasets (e.g. Braitenberg et al., 2000a, 2000b, 2006, 2008; Ebbing et al. 2007; Oakey and Stephenson, 2008; Aitken et al., 2009, 2013; Aitken, 2010; Mazur et al., 2012; Van der Meijde, 2013; Steffen et al., 2011, 2017). The 3D inverse modelling of BA grid data has been conducted, in this study, using the LithoFLEX 2.0 software package (Braitenberg et al., 2008; Braitenberg, 2012). The LithoFLEX 2.0 software package implements and/or utilises the inversion algorithm by Parker and Oldenburg (Parker, 1972; Oldenburg, 1974) and uses the following input parameters: BA grid data, reference depth, density contrast and cut-off wavelength, in order to estimate the morphology/depths of a single layer interface (e.g. Moho) during the modelling task.

The approach adopted during the 3D inverse modelling, in order to accurately determine the morphology/depths of Moho, include:

1. Selection of BA grid data larger (wider) than the present study area (shown in Figure 2) in order to give adequate control on regional structures (e.g. Moho) and their responses as well as to avoid edge effects on the Moho depths. The spatial size of the selected area spans from longitudes 7º 00' E to 11º E and latitudes 6º N to 10º N (see Figure 1 for location).
2. Assigning a reference depth to the crust-mantle interface (Moho). The reference depth, which represents the average Moho depth beneath the area, is set to 27 km (i.e. 27000 m) and was determined beforehand from spectral analysis of BA grid data (cf. Figure 3d) as well as from

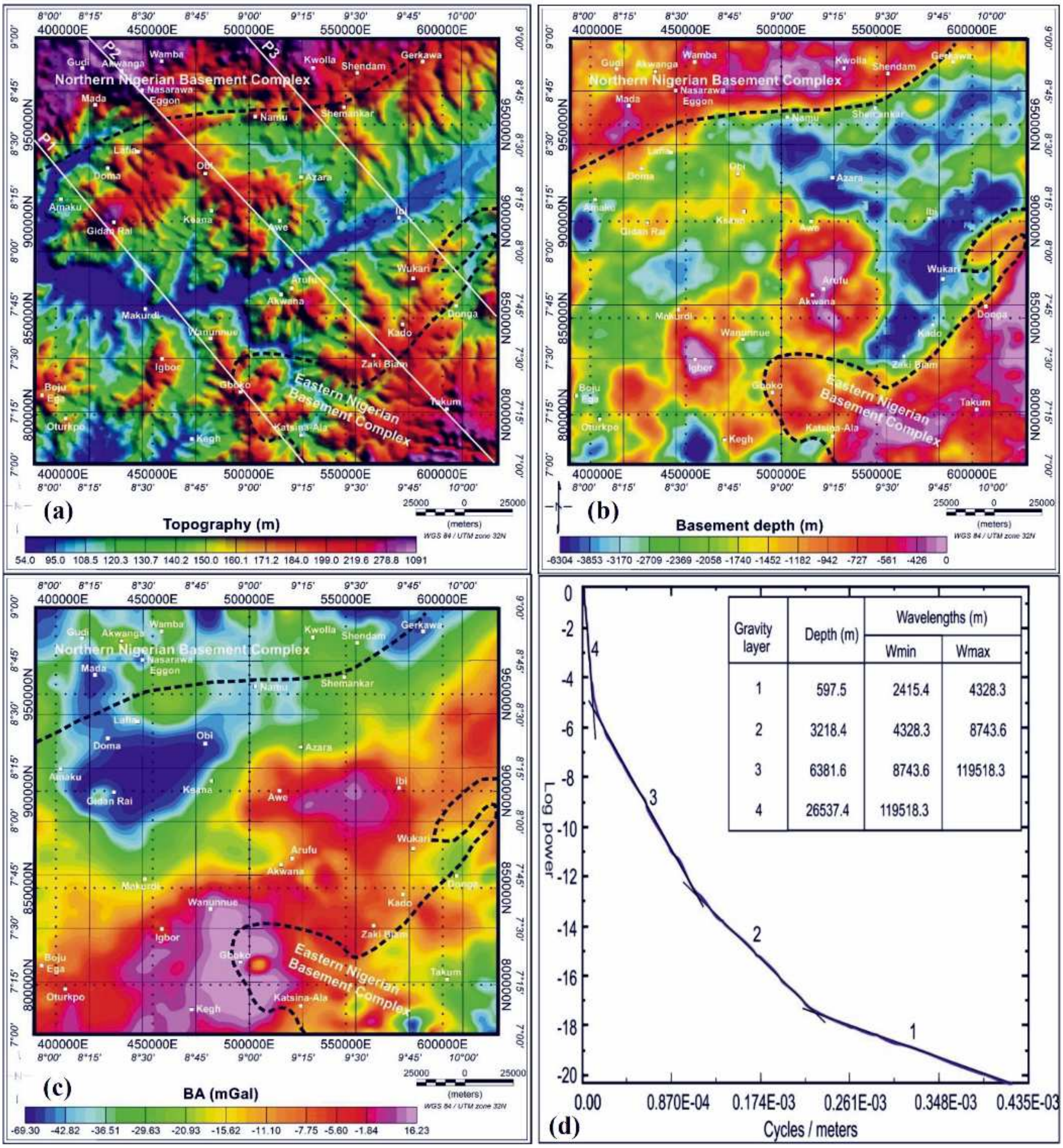

Fig 3: (a) Topography map of the study area. Note that the three NW-SE profiles (P1 – P3; thick white lines) shown on the topography map were used in this present study for the comparison of predicated Moho depths with the corresponding topography and Bouguer gravity anomaly values as well as in the generation of two dimensional (2D) crustal structures across the area. (b) Depth to basement (sediment thickness) map adopted from the basement depth grid data of Anudu (2017) and Anudu et al. (2020). (c) Bouguer gravity anomaly (BA) map. (d) Spectral analysis result of the Bouguer gravity anomaly (BA) grid data spectrum; the gravity layer of interest, in this figure d, is the layer number 4 which is associated with the underlying Moho structures and therefore, a low-pass filter with a cut-off wavelength of 120000 m (120 km) was selected (which corresponds to Bouguer gravity anomalies originating at an average depth of about 26537 m) to emphasise/accentuate the longer-wavelength anomalies due to Moho in the BA map of the area, as discussed in this paper.

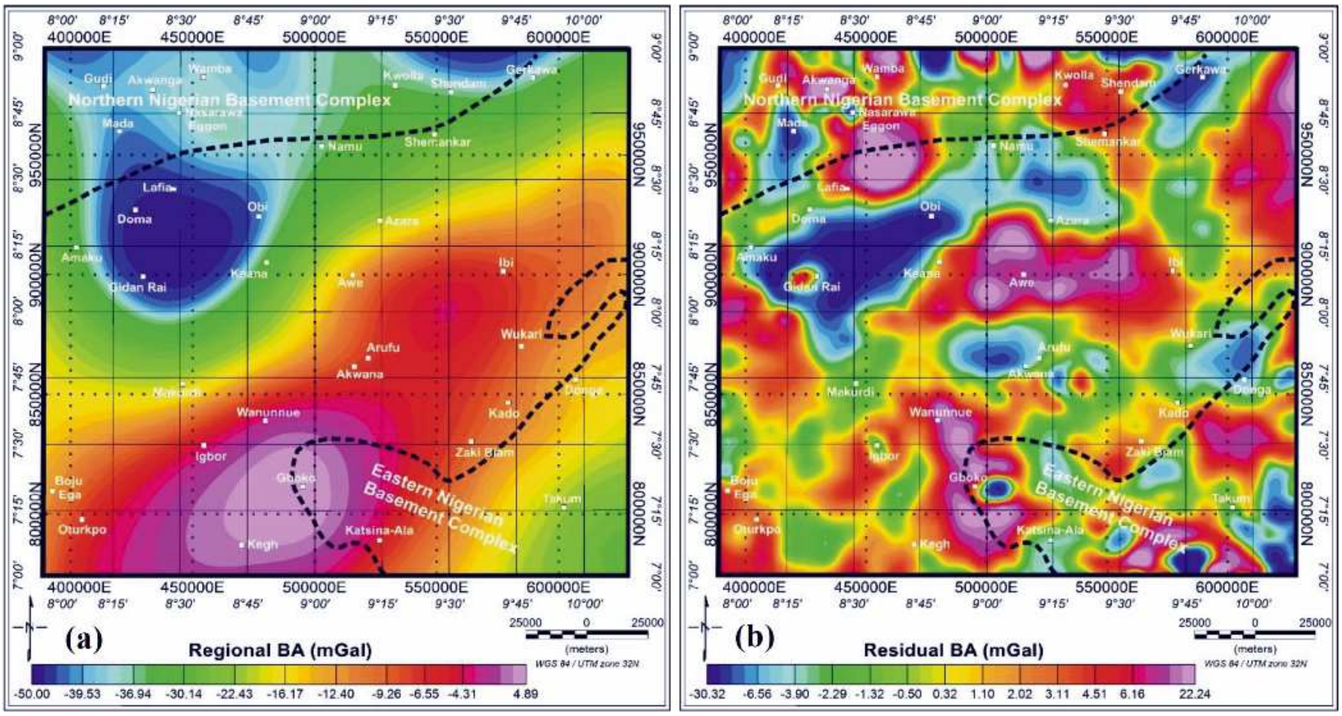

Fig. 4: (a) Regional Bouguer gravity anomaly (regional-BA map), and (b) residual Bouguer gravity anomaly (residual-BA) map. Both figures were produced from the spectral analysis result of the Bouguer gravity anomaly (BA) grid data spectrum.

published nearby seismic refraction (Stuart et al., 1985) and teleseismic (Tokam et al., 2010; Gallacher and Bastow, 2012; Akpan et al., 2016) Moho depth results. It represents the average Moho depth beneath the area.

3. Assigning a density contrast between the crust and mantle. The density contrast is set to 0.3 g/m^3, after testing several standard density contrast ranges of 0.2 – 0.5 g/m^3.
4. Selection of cut-off wavelength for the Hanning low-pass filter to be used in the removal of shorter-wavelength anomalies (signals) emanating from shallow crustal (upper-crustal) bodies with different densities, so as to emphasis the longer-wavelength anomalies (signals) required in assessing the Moho. The cut-off wavelength is set to 120 km and was also determined beforehand from spectral analysis of BA grid data (cf. Figure 3d). However, other wavelengths (80, 100, 110 and 130 km) were also tested but generated somewhat similar results.
5. Examining and refining the derived Moho depths by varying the input parameters for the 3D inverse modelling of the BA grid data, as well as comparing them with the previously published Moho depths from nearby seismic refraction (Stuart et al., 1985) and teleseismic (Tokam et al., 2010; Gallacher and Bastow, 2012; Akpan et al., 2016) studies.
6. Varying the input parameters for the 3D inverse modelling of the BA grid data in order to examine their effect on the result as well as to ascertain an estimate of uncertainty in the final Moho depths.
7. The accepted final predicated Moho depths/model presented in Figure 5a, which is considered the most reasonable Moho depth values, is produced with a 27 km reference depth, 0.3 g/m^3 density contrast and 120 km low-pass filter cut-off wavelength. It was regarded to be the most reasonable because it is in good agreement with previous Moho depth estimates from nearby seismic/teleseismic studies (Stuart et al., 1985; Tokam et al., 2010; Gallacher and Bastow, 2012; Akpan et al., 2016) and also it was generated with the parameters derived previously from the spectral analysis of the Bouguer gravity anomaly data grid; cf. Figure 3d). Estimated uncertainties (errors) in the final Moho depths is ± 2 to 3 km. Furthermore, a 3D perspective view of the final predicated Moho model for the study area is shown in Figure 5b, and it highlights further the striking variations in Moho morphology across the area.

Also comparisons of the derived Moho depths with the topography (terrain elevation) and Bouguer gravity anomaly values were conducted utilising three profiles (labelled P1 – P3) (Figure 6), from the appropriate respective grids (cf. Figures 3a, 3c and 5), to throw more light on their relationships across the area.

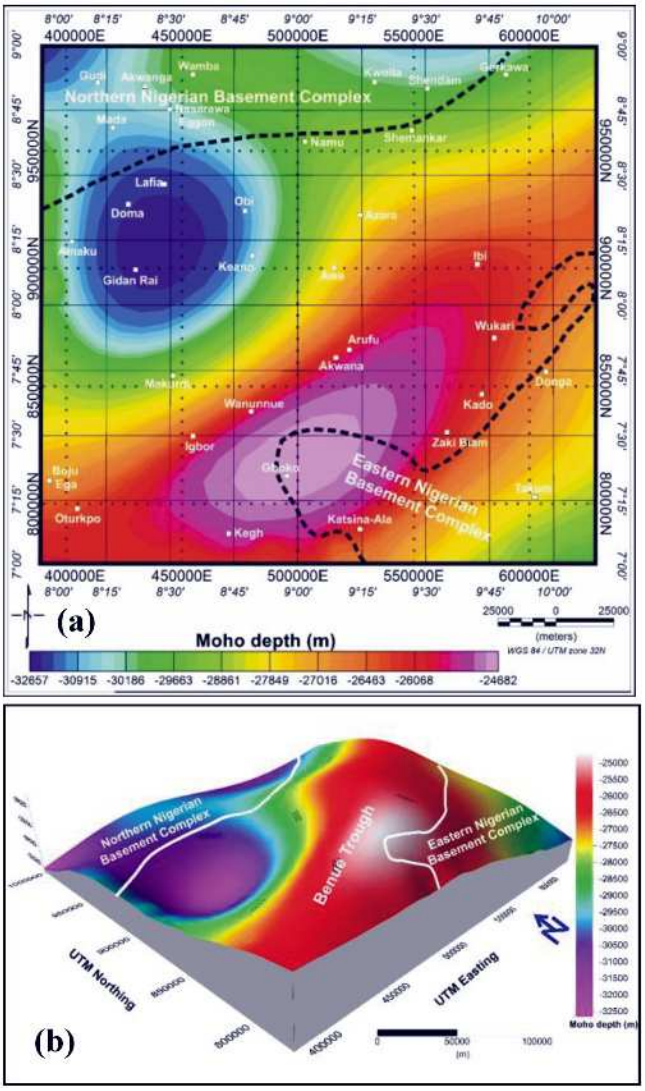

Fig. 5: (a) Predicated Moho depth model/map derived from the three-dimensional (3D) inverse modelling of the Bouguer gravity anomaly (BA) results for the study area. (b) 3D perspective view of the predicated Moho depth model; it gives an impressive visual view of the Moho morphology/geometry across the area. Both figures indicate that the morphology/geometry of Moho structures underlying the Trough exhibits a general northeast-southwest (NE-SW) trend strikingly similar to the trends of the broad, long-wavelength axial positive anomalies observed on both the BA and regional-BA maps. They further depict that the Trough axial region are characterised by elevated Moho structures (shallow Moho depths).

In addition, the crystalline crustal thickness grid of the area (shown in Figure 7a) was determined by simply subtracting the basement depth (sediment thickness) grid (Figure 3b) from the Moho depth grid (Figure 5a). This approach has been employed by a number of seismic and/or gravity studies in the estimation of crystalline crustal thickness values in different geological and/or tectonic settings (such as continental rifts, passive margins) around the world (e.g. Oakey and Stephenson, 2008; Mazur *et al*., 2012; Fairhead, 2015; Anudu, 2017; Kusznir *et al*., 2018). Furthermore from the resulting crystalline crustal thickness grid, the crustal stretching factor (β) grid of the area (presented in Figure 7b) was generated utilising a reference crustal thickness of 33 km (i.e. 33 km thick unstretched crust prior to rifting) as seismically imaged by Stuart *et al*. (1985), Tokam *et al*. (2010), Gallacher and Bastow (2012) and Akpan *et al*. (2016) for the basement complex terrains close to the study area (cf. Figure 1). This aforementioned method has been used by several seismic and/or gravity studies in the determination of crustal stretching factor (β) values across the world (e.g. Su *et al*., 1989; Tiberi *et al*., 2005; Maguire, *et al*. 2006; Mazur *et al*., 2012; Allen and Allen, 2013; Ahmed, 2014; Anudu, 2017).

Results and Discussion

Semi-Quantitative Interpretation of the Topography

The topography map (Figure 3a) shows that the variation in terrain elevations across the region is a product of regional tectonic activities and geology. The Trough region underlain by Cretaceous sedimentary rocks, that had been intruded by numerous (Late Cretaceous – Palaeogene) magmatic (volcanic/sub-volcanic and intrusive) rocks of mafic to intermediate composition (cf. Offodile, 1976, 1980, 1989; Adighije, 1981; Umeji, 1985, 2000; Benkhelil et al., 1988; Benkhelil, 1989; Obiora, 2002; Nwajide, 2013; Anudu et al. 2014; 2020; Anudu, 2017; Figure 2), is characterised by elevations in the range of 50 to 230 m above sea level with the exception of a smaller area around Gidan Rai with altitude of more than 406 m (Figure 3a). Lower elevations occur mostly along the river channels (of the Benue River, Mada River, Dep River and Kastina-Ala River), with the lowest value (c. 50 m) observed on the western end of the Benue River channel (Figure 3a). In contrast, the basement complex regions are mostly characterised by elevations greater than 250 m with average values between 250 and 550 m (cf. Figure 3a). The highest elevations (550 – 1100 m) occur around Mada – Nasarawa Eggon – Akwanga – Wamba areas that correspond to the position of the high-level anorogenic, Jurassic Younger Granite ring complex that intruded the low-lying Precambrian basement rocks of the Northern Nigerian Basement Complex situated in the northwestern region, as well as around Takum area in the southeastern region which is situated within the Eastern Nigeria Basement Complex, an eastern portion of the uplifted Adamawa Massif (Figures 2 and 3a).

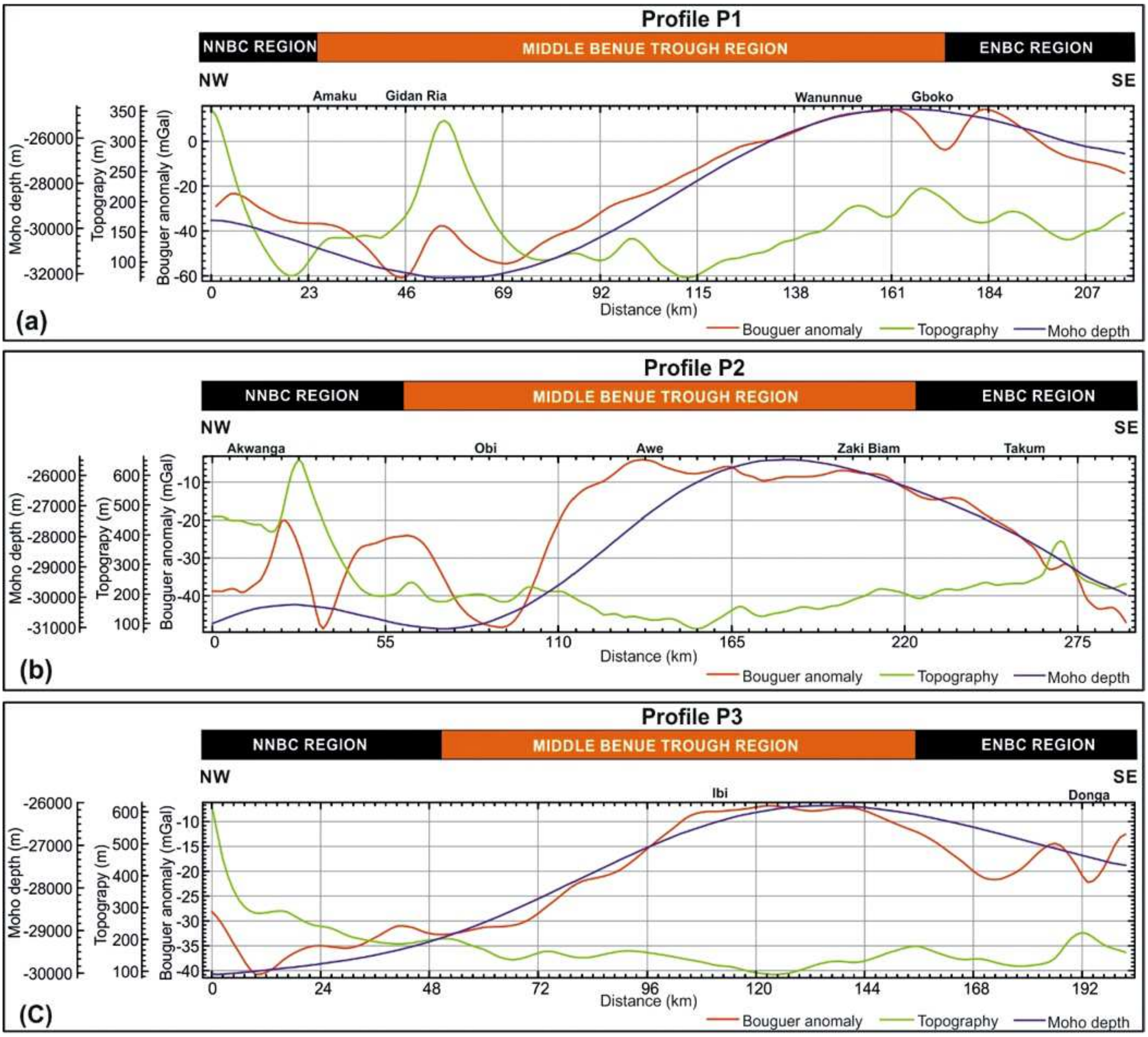

Fig. 6: Comparison of Moho depths with the topography and Bouguer gravity anomaly values along three NW-SE profiles (P1 - P3) in the study area. (a) Profile P1, (b) Profile P2 and (c) Profile P3. Topography (green line), Bouguer gravity anomaly (red line) and Moho depth (blue line) values were extracted along these aforementioned three profiles from their respective grids/maps (Figures 3a, 3c and 5a). This figure shows that areas with deeper Moho depths are typically associated with higher topography reliefs and broader longer-wavelength negative Bouguer gravity anomalies, whereas those with shallower Moho depths are generally associated with lower topography reliefs and broader longer-wavelength positive to near-positive Bouguer gravity anomalies. NNBC = Northern Nigerian Basement Complex, and ENBC = Eastern Nigerian Basement Complex. Names of cities/towns very close to the profile locations are also shown. Locations of profiles are shown in Figure 3a.

Semi-Quantitative Interpretation of the Bouguer Gravity Anomalies

The BA map (Figure 3c) shows that smaller shorter-wavelength and broader longer-wavelength, positive to near-positive anomalies generally characterised the axial region of the Trough, whereas a broader negative anomaly occurs over the Trough northwestern region (Obi – Gidan Rai areas). It also reveals that the adjoining (Precambrian) basement complex regions are largely characterised by broader, longer-wavelength negative anomalies (Figure 3c). These aforementioned anomalies are greatly highlighted on either the regional-BA map (Figure 4a) or residual-BA map (Figure 4b) as the case may be and thus, are further interpreted utilising both maps.

The regional-BA map (Figure 4a) reveals more clearly

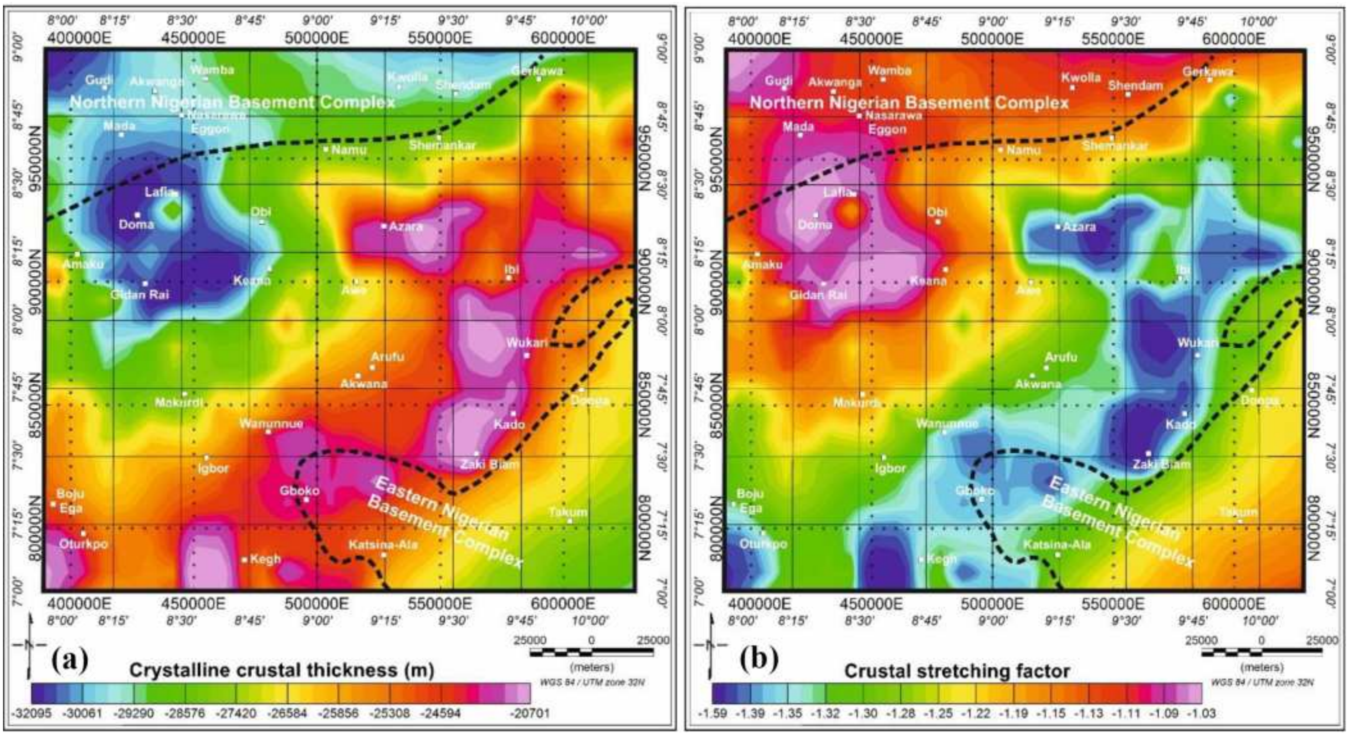

Fig. 7: (a) Predicated crystalline crustal thickness map; it was generated by subtracting the basement depth grid of Anudu (2017) and Anudu et al. (2020) (Figure 3b) from the predicated Moho depth model grid (Figure 5a) derived from the 3D inverse modelling of BA. (b) Predicted crustal stretching factor (β); it was produced by dividing the reference crustal thickness of 33 km (as seismically estimated to be the original thickness of unstretched crust prior to rifting; e.g. Stuart *et al.*, 1985) by the predicated crystalline crustal thickness grid obtained in this study (Figure 7a).

the presence of (extensive) broader, NE-SW to ENE-WSW orientated, longer-wavelength positive to near-positive and negative anomalies with amplitudes and widths greater than 20 mGal and 140 km, respectively, across the study area. These broader, longer-wavelength anomalies (whether positive to near-positive or negative) typically reflect the variations in lateral densities across deeper large-scale crustal features, and are, in this study, interpreted to be associated with the Moho and upper mantle bodies as well as crustal thickness variations across the area. Furthermore, based on the Airy compensation mechanism (cf. Hinze et al., 2013; Long and Kaufmann, 2013; Anudu, 2017), two interpretations are made: (1) the broader, longer-wavelength positive to near-positive anomalies along the axial region of the Trough (Figure 4a) indicate the presence of thinner crust, shallower Moho and, probably, isostatic effect of lower topography; (2) the broader, longer-wavelength negative anomalies over the adjoining crystalline basement complexes as well as the Trough northwestern region (Obi – Gidan Rai areas) (Figure 4b) reflect the presence of thicker crust, deeper Moho and isostatic effect of higher topography. These interpretations are supported by published gravity (Cratchley and Jones, 1965; Adighije, 1978, 1979, 1981a; Osazuwa et al., 1981; Fairhead and Okereke, 1987; Okereke, 1988; Anudu, 2017), seismic refraction (Stuart et al., 1985) and teleseismic (Akpan et al., 2016) studies in the Benue Trough and adjoining basement complex regions. Additionally, the broader longer-wavelength negative anomalies with amplitude of up to -28 mGal in the Trough northwestern region (around Obi – Gidan Rai areas) may also be related to shallower to deeper crustal flexural responses, since this particular area is situated between a high and low (synclinal) topographic features (cf. Figures 3a and 4a).

The residual-BA map (Figure 4b) greatly highlights numerous smaller, shorter-wavelength, positive to near-positive anomalies across the Trough axial region. These shorter-wavelength, axial positive to near-positive anomalies generally coincide with many locations where numerous (mafic to intermediate) magmatic rocks have been identified/mapped through field geological (cf. Offodile, 1976, 1980, 1989; Adighije, 1981; Umeji, 1985, 2000; Benkhelil et al., 1988; Benkhelil, 1989; Obiora, 2002; Nwajide, 2013) and magnetic (cf. Anudu et al., 2014; 2020; Anudu, 2017) studies (compare Figure 2 and 4b). They also generally coincide with locations having several uplifted basement ridges and/or shallow magnetic basement depths (cf. Anudu, 2017; Anudu et al., 2020; cf. Figure 3b) as well several occurrences of dense hydrothermal mineral deposits (e.g. galena, sphalerite, and barite) (cf. Offodile, 1980; Wright et al., 1985; Akande et al., 1989). Thus, these shorter-wavelength, axial positive to near-positive anomalies generally reflect the lateral density variations within the shallower upper crustal region and are interpreted to be associated with occurrences of dense intra-sedimentary/intra-crustal magmatic rocks, uplift basement ridges/horsts and dense hydrothermal mineral deposits (e.g. galena, sphalerite, and barite) within the Trough axial region. Also, several localised, shorter- to intermediate-wavelength, negative anomalies observed over the Trough and adjacent basement complexes on the residual-BA map (Figure 4b) are mainly associated with the occurrences of (low density) granites, granitic rocks and felsic gneisses in these regions. This interpretation is supported by published field geological studies which showed the presence of numerous Pan-African granites, Jurassic younger granites, Precambrian felsic gneisses and granitic gneisses (of the Migmatite-Gneiss Complex) within these regions (e.g. Woakes et al., 1987; Rahaman, 1989; Obaje, 2009; NGSA, 2009; Nwajide, 2013; Anudu, 2017).

Moho Depth Model

The predicated Moho depth model/map (Figure 5a) and its 3D perspective view (Figure 5b) clearly show prominent lateral variations in the estimated Moho depths and hence, they strongly reveal remarkable changes in the Moho morphology across the study area. They also reveal a striking elongated (ridge-like), shallow (elevated) Moho structures orientated approximately NE-SW beneath the entire axial region of the Trough (cf. Figure 5). The position and orientation of this Moho structures coincide remarkably well with the Trough axial region characterised by broader, NE-SW trending, longer-wavelength positive to near-positive anomalies in both the BA map (Figure 3c) and regional-BA map (Figure 4a); thus, it clearly indicates that the broader, NE-SW trending, longer-wavelength positive to near-positive Bouguer gravity anomalies observed along the Trough axial region are strongly associated with this elongated, shallow (uplifted/elevated) Moho structures imaged in this study. This interpretation is in good agreement with the semi-quantitative interpretation of the Bouguer gravity anomalies previously made in sub-section 4.2.

The Moho depths are shallower along the Trough axial region, and deeper beneath the adjoining Northern and Eastern Nigerian Basement Complex regions as well as the Trough northwestern region (Figure 5). Generally, the Moho depths range between c. 24 ± 2 and 32 ± 3 km (Figure 5). The shallowest Moho depths (c. 24 ± 2 to 26 ± 3 km deep) are found in and around the Gboko – Igbor – Wanunne – Kegh – Akwana – Wukari areas within the Trough axial region (Figure 5) which are typically characterised by lower topography reliefs (Figure 3a), broader longer-wavelength positive to near-positive Bouguer gravity anomalies (Figures 3c and 4a), and are also strongly affected by the rifting events. This indicates that there has been a large amount of crustal and/or lithospheric extension in the axial region of the Trough. The deepest Moho depths (c. 28 – 32 ± 3 km deep) occur beneath the Trough northwestern region (e.g. Gida Rai, Amaku, Doma, Lafia, Obi, Keana), Northern Nigerian Basement Complex region (e.g. Mada, Gudi, Akwanga, Nasarawa Eggon, Kwolla and Shendam) and the southeastern end (e.g. Takum) of the Eastern Nigerian Basement Complex region (Figure 5); these above-mentioned areas typically exhibit higher topography reliefs (Figure 3a), broader longer-wavelength negative Bouguer gravity anomalies (Figures 3c and 4a), and are also generally less affected by the rifting events.

Furthermore, these aforementioned Moho depths, obtained in this study, are in good agreement with (and/or comparable to) those determined in the adjoining lower (Akpan et al., 2016) and upper (Stuart et al., 1985; Fairhead and Okereke, 1987, 1990; Okereke, 1988; Tokam et al., 2010) Benue Trough regions, as well as the flanking basement complex regions (Stuart et al., 1985; Tokam et al., 2010; Gallacher and Bastow, 2012; Akpan et al., 2016). Recent teleseismic studies by Akpan et al. (2016) derived Moho depths of c. 22 – 23 km underneath the lower Benue Trough and c. 33 – 35 km beneath the unrifted adjacent basement complexes, far away from the Trough (Figure 1). Also seismic refraction (cf. Stuart et al., 1985), gravity (cf. Fairhead and Okereke, 1987, 1990; Okereke, 1988) and teleseismic (cf. Tokam et al., 2010; Gallacher and Bastow, 2012) studies conducted in and across the upper Benue Trough (particularly in its Yola/Garoua Rift area) estimated Moho depths of c. 23 – 25 km beneath the rift basin area and c. 30 – 35 km across the unrifted adjoining basement complex areas (cf. Figure 1).

Comparisons of Moho Depth with Topography and Bouguer Gravity Anomaly Using Profiles

In this section, the derived Moho depths were compared with the topography and Bouguer gravity anomaly (BA) values along three selected profiles (labelled P1 – P3; Figure 6), to throw more light on their relationships across the area. Profiles were constructed to transect the

Trough and the adjoining Northern and Eastern Nigerian Basement Complex regions. Position of the three profiles (labelled P1 – P3) are shown in Figure 3a and the respective Moho depth, topography and BA values extracted along these aforementioned three profiles are presented in Figure 6. The aforementioned Figure 6 clearly further highlights that the observed broad, axial longer-wavelength near-positive Bouguer gravity anomalies over the Trough are strongly associated with elevated (shallow) Moho and isostatic effect of lower topography, whereas the large longer-wavelength negative anomalies across the surrounding basement complexes and northwestern region of the Trough (Obi – Gidan Rai areas) are largely due to deep Moho and isostatic effect of higher topography. The above-mentioned information obtained from the comparisons of Moho depths with the topography and BA values along these three profiles is strongly in agreement with the well-known Airy compensation model (cf. Hinze et al., 2013; Long and Kaufmann, 2013; Anudu, 2017).

Crystalline Crustal Thickness Model

The predicated crystalline crustal thickness model/map (Figure 7a) strongly shows a remarkable lateral variations in the crystalline crustal thickness across the study area, and these variations are products of regional tectonic activities and geology. The crystalline crustal thickness values are smaller beneath the Trough axial region which were strongly affected by the rifting events, and larger underneath the adjoining Northern and Eastern Nigerian Basement Complex regions as well as the Trough northwestern region (Figure 7a) which were less affected by the rifting events. In general, the crystalline crustal thickness values across the study area vary from c. 20 ± 2 to 32 ± 3 km. The thinnest crystalline crust (c. 20 – 24 ± 2 km thick) is found beneath five sedimentary sub-basins (Azara-Shemankar Sub-basin, Wukari-Zaki Biam Sub-basin, Wanunnue Sub-basin, South Oturkpo Sub-basin, and South Kegh Sub-basin), recently identified/mapped from detailed magnetic studies (cf. Anudu, 2017; Anudu et al., 2020), located within the Trough axial region (cf. Figures 3b and 7a). Thus, this shows that the maximum thinning of the crust (and/or the lithosphere) occurs beneath these aforementioned sub-basins areas. Also it reveals that the areas of maximum crustal thinning (and/or lithospheric thinning) coincide with those of uplifted (elevated) shallow Moho within the Trough axial region (compare Figures 5 and 7a), and therefore, strongly indicates that the main rift axis of the Trough lies within this region. Moderately thin crystalline crust (c. 25 – 27 ± 3 km) occurs beneath the north, northwest and southeast areas located few kilometres away from the Trough axial region (Figure 7a). The thickest crystalline crust (c. 28 – 32 ± 3 km thick) occurs beneath the Trough northwestern region, Northern Nigerian Basement Complex and southeast area of the Eastern Nigerian Basement Complex (Figure 7a), similar to the deepest Moho, where the surface topography reliefs exceed 250 m and the longer-wavelength Bouguer gravity anomalies are generally negative (cf. Figure 5). This finding is in good agreement with the semi-quantitative interpretation of the BA map (Figure 3c) and regional-BA map (Figure 4a) (cf. sub-section 4.2) and, furthermore, it is generally consistent with Airy-type compensation model that suggests thickening of the crust caused by the isostatic adjustment resulting from higher topography (Hinze et al., 2013; Long and Kaufmann, 2013; Anudu, 2017).

Furthermore, the above-mentioned crystalline crustal thickness values obtained in this study are consistent with crustal thickness estimates of c. 18 – 35 km identified underneath the Trough and its flanking basement complex regions by previous seismic refraction (cf. Stuart et al., 1985), gravity (cf. Fairhead and Okereke, 1987, 1990; Okereke, 1988; Anudu, 2017) and teleseismic (cf. Tokam et al., 2010; Gallacher and Bastow, 2012; Akpan et al., 2016) studies.

Crustal Stretching Factor Model

The predicated crustal stretching factor (β) model/map (Figure 7b) reveals a sufficiently great lateral variation in the crustal stretching factor (β) values across the study area. The crustal stretching factor (β) varies from c. 1.03 within the Trough northwestern area and adjoining basement complex regions to c. 1.59 in the Trough axial area (Figure 7b). Thus, this study, shows that the study area generally exhibits moderately high crustal stretching factor (β) which resulted from the cumulative effects of several extensional and wrench (strike-slip) tectonics associated with past rifting events that have strongly affected the crust/lithosphere beneath Trough. Also, it indicates that the crystalline crust and/or the entire lithosphere beneath the Trough axial region (particularly in the sedimentary sub-basins areas) has undergone significant stretching. The moderately high stretching factor (β) values combined with available geological information suggest that the Trough is likely to be characterised by numerous, relatively high to moderate angle normal faults and strike-slip faults with several associated sub-basins and uplifted, faulted crustal basements. This interpretation is in agreement with results from detailed magnetic studies in the area (Anudu, 2017; Anudu et al., 2020) and field (outcrop) geological studies in contiguous upper and lower Benue Trough segments (Maurin et al., 1986; Benkhelil, 1989; Guiraud, 1990; Guiraud and Maurin, 1992; Wilson and Guiraud, 1992), as well as seismic studies (Avbovbo et al., 1986; Suleiman et al., 2017) in the Bornu Basin to the northeast (cf. Figure 1), which is genetically associated with the Benue Trough. In addition, the crustal stretching factor (β) values indicate that maximum crustal thinning occurred primarily within the Trough axial region, suggesting a good correlation of maximum crustal stretching region with the uplifted (elevated) shallow Moho region. Furthermore, the crustal stretching factor values (β = c. 1.03 – 1.59) obtained in this study are in good agreement with (and/or comparable to) those determined in several continental rift basins across the world, particularly the Main Ethiopian Rift within the East African rift system (β = c. 1.2 – 2.0, Tiberi et al., 2005; β = c. 1.1 – 1.7, Maguire, et al. 2006).

Two-Dimensional Crustal Structure Models

In the section, two-dimensional (2D) crustal structure models (Figure 8) along the previously selected three profiles (labelled P1 – P3) were produced to further highlight the morphology/geometry of shallow crustal basement (cf. Anudu (2017; Anudu et al., 2020) and the Moho, as well as their relationships across the area. The shallow crustal basement and the Moho depth values along the three profiles were extracted from the basement depth (sediment thickness) grid map (cf. Anudu, 2017; Anudu et al., 2020; Figure 3b) and the Moho depth map (Figure 5), respectively, and the results are shown in Figure 8.

The Figure 8 reveals that several sedimentary sub-basins (depocentres), shallow (uplifted) faulted crustal basements, shallow Moho and thin crystalline crust characterised the Trough axial region and these features are interpreted to have been formed through (regional) extensional tectonics associated with rifting events which affected the underlying crust/lithosphere in the Early to Late Cretaceous. It can also be observed that shallow (elevated) Moho depths occur beneath most of the imaged sedimentary sub-basins areas found across the Trough axial region and thus indicates that the areas with shallowest Moho coincide with areas of maximum basin depths where the crust is thinnest. Also it shows that the zone of crustal thinning coincides with zone of crustal basement faulting across the Trough (Figure 8). Furthermore, the Figure 8 also reveals that the geometry of the thinned crust obtained in this study is typically consistent with ductile necking and the near-uniform to uniform stretching of the crust/lithosphere (cf. Anudu, 2017). All of the above-mentioned features and/or observations seem to be more characteristic of, or compatible with, the well-known McKenzie (1978) extensional rift basin model (i.e. McKenzie model) in which lithosphere extension (stretching) is by brittle failure (faulting) in the upper crust and ductile flow (distributed plastic deformation) in the lower crust and upper mantle. This interpretation is in good agreement with several studies conducted across the Benue Trough (cf. Fairhead and Green, 1989; Fairhead and Okereke, 1987, 1990) and other genetically-related intracratonic rift basins referred to as the West and Central African Rift Systems (WCARS; cf. Bermingham et al., 1983; Fairhead and Green, 1989; Mohamed et al., 2001; Fairhead et al., 2013).

Tectonic and Geodynamic Implications

The Moho and crystalline crust structures imaged within and/or beneath the Trough axial region exhibit a major NE-SW trend (Figures 5 and 7a) which is strikingly similar to the trend/orientation of the Benue Trough, the offshore Chain and Charcot oceanic fracture zones (cf. Figure 1) as well as structures (cf. Figure 2b) mapped from detailed magnetic studies by Anudu et al. (2014) and Anudu (2017). Thus, the imaged NE-SW orientated Moho and crystalline crust structures strongly indicate that a major NW-SE regional extensional tectonic stress field coupled with a NE oriented transcurrent stress components were more dominant at the time of stretching and/or rifting across the middle Benue Trough region during its geological evolution (cf. Anudu et al., 2020). Additionally, the NE-SW major trend of the Moho and crystalline crust structures is similar to the trend of major regional faults, fracture systems and shear zones (mostly Pan-African in age) observed in the field across the Trough and surrounding basement complexes of Nigeria (e.g. Rahaman et al., 1984; Maurin et al., 1986; Ajibade et al., 1989; Ajibade and Wright, 1989; Benkhelil et al., 1989; Guiraud et al., 1989; Rahaman, 1989; Obaje, 2009; Anudu, 2017; Anudu et al., 2020); this implies that the major pre-existing tectonic fabrics or zones of weakness (Late Pan-African in age) within the underlying crustal basement/crust/lithosphere across the study area generally exhibit a dominant NE-SW regional trend and are thought to have controlled the orientation of the Benue Trough and its internal structures (cf. Anudu, 2017; Anudu et al., 2020). Furthermore, the areas with shallow Moho structures/depths and/or thin crystalline

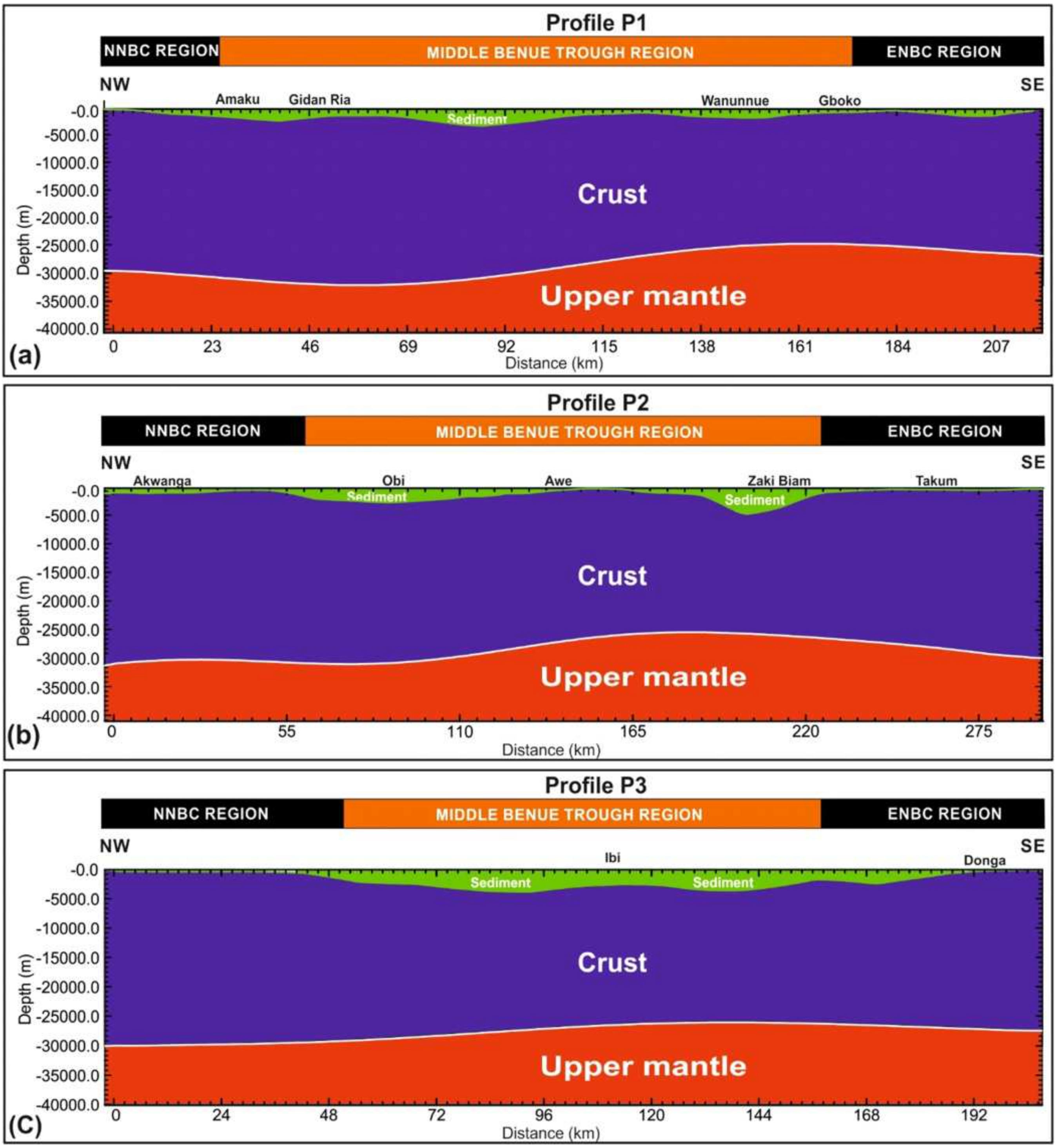

Fig. 8: Two-dimensional (2D) crustal structure along three NW-SE profiles (P1 - P3) in the study area. (a) Profile P1, (b) Profile P2 and (c) Profile P3. The respective profiles were extracted from both the depth to basement (sediment thickness) map (cf. Figure 3b) of Anudu (2017) and Anudu et al. (2020) and the Moho depth map (cf. Figure 5a). White line represents the Moho (crust-upper mantle interface) depths along profiles. The figure clearly shows the variations in crustal basement morphology and Moho topography/geometry across the middle Benue Trough and adjoining regions. NNBC = Northern Nigerian Basement Complex, and ENBC = Eastern Nigerian Basement Complex. Names of cities/towns very close to the profile locations are also shown. Locations of profiles are shown in Figure 3a.

crust coincide remarkably well with areas intruded by numerous (mafic to intermediate) magmatic rock bodies which have been mapped from field geological works (cf. Offodile, 1976, 1980, 1989; Adighije, 1981; Umeji, 1985, 2000; Benkhelil et al., 1988; Benkhelil, 1989; Obiora, 2002; Nwajide, 2013) and detailed magnetic studies (cf. Anudu et al., 2014; 2020; Anudu, 2017) across the Trough axial region (Figure 9). The coincidence of these areas underlain by shallow Moho structures/depths and/or thin crystalline crust with those having numerous magmatic rock bodies and structures (as shown in Figure 9) suggest that melts accompanying the tectonic extension of the crust/lithosphere and passive upwelling of mantle materials during the Trough's evolution seems to have followed several deep-reaching, pre-existing crustal discontinuities (e.g. faults/fracture systems) of (mainly) Pan-African age that have been reactivated at various geological times (cf. Maurin et al., 1986; Fairhead and Green, 1989; Ziegler and Cloetingh, 2004; Cloetingh et al., 2015; Anudu, 2017).

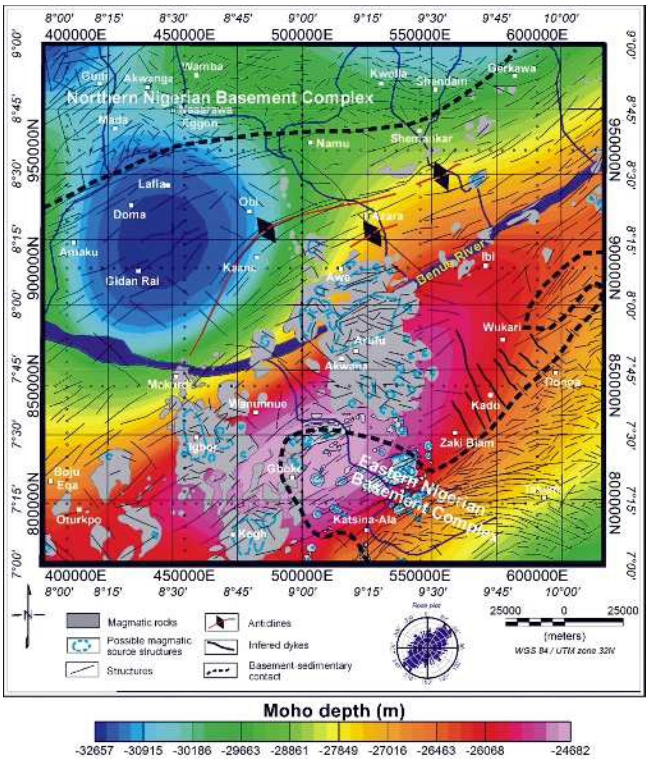

Fig. 9: Map showing the relationship between the shallow Moho structure/depths and areas of magmatic rock bodies in study area. It clearly reveals that the areas underlain by shallow Moho structure/depths (and/or thin crystalline crust) coincide remarkably well with areas intruded by numerous (mafic to intermediate) magmatic rock bodies. It was produced by superimposing the magmatic rock and structural distribution map derived from the detailed magnetic studies (after Anudu et al., 2014; Anudu, 2017; cf. Figure 2b) on the predicated Moho depth model/map (cf. Figure 5a) of the area.

Summary and Conclusions

The topography and BA maps show that the variations in terrain elevations and Bouguer gravity anomalies, respectively, across the study area are products of regional tectonic activities and geology.

Regional-residual BA separation was done employing wavelength filtering method based on the result derived from spectral analysis of the BA data grid. The 3D inversion applied to the satellite BA grid data reveals remarkable lateral variations in Moho depths and/or Moho morphology beneath the study area. The imaged Moho depths vary from c. 24 ± 2 to 32 ± 3 km across the study area, with the shallowest Moho depths (c. 24 – 26 ± 2 km deep) occurring beneath Gboko – Igbor – Wanunne – Kegh – Akwana – Wukari areas within the Trough axial region. The crystalline crustal thickness values computed range between c. 20 ± 2 and 32 ± 3 km with the thinnest crystalline crust (c. 20 – 24 ± 2 km thick) found beneath five sedimentary sub-basins (Azara-Shemankar Sub-basin, Wukari-Zaki Biam Sub-basin, Wanunnue Sub-basin, South Oturkpo Sub-basin, and South Kegh Sub-basin) located within the Trough axial region. The crustal stretching factor (β) values vary from c. 1.03 to 1.59 with smaller values (β = c. 1.03 to 1.25) occurring within the Trough northwestern area and adjoining basement complex regions and larger values (β = c. 1.26 to 1.59) in the Trough axial area. The imaged Moho and crystalline crust structures beneath the Trough axial region exhibit a major NE-SW orientation which is strikingly similar to the orientation of the Benue Trough, structures and regional Bouguer gravity anomalies. Also this study reveals that the shallow faulted crustal basements, shallow Moho and thin crystalline crust that characterised the Trough axial region were mainly formed through (regional) extensional tectonics which affected the underlying crust/lithosphere during rifting events in the Early to Late Cretaceous.

Acknowledgements

We thank the Bureau Gravimétrique International (BGI) France for releasing the Satellite Bouguer gravity data utilised in this study.

References

Adighije, C.I. (1978). Studies of the gravity field of the Benue Trough of Nigeria. Ph.D. Thesis, University of Ibadan, Nigeria. (Unpublished).

Adighije, C.I. (1981a). A gravity interpretation of the Benue Trough, Nigeria. Tectonophysics, Vol. 79, pp. 109-128.

Adighije, C.I. (1981b). Gravity study of lower Benue Trough Nigeria. Geological Magazine, Vol. 118, No. 1, pp. 59-67.

Ahmed, A., Leroy, S., Keir, D., Korostelev, F., Khanbari, K., Rolandone, F., Stuart, G. and Obrebski, M. (2014). Crustal structure of the Gulf of Aden southern marg*In:* Evidence from receiver functions on Socotra Island (Yemen). Tectonophysics, Vol. 637, pp. 251-267.

Aina, A., Olorunfemi, M.O. and Ojo, J.S. (1996). An integration of aeromagnetic and electrical resistivity methods in dam site investigation. Geophysics, Vol. 61, No. 2, pp. 349-356.

Aitken, A.R.A. (2010). Moho geometry gravity inversion experiment (MoGGIE): a refined model of the Australian Moho, and its tectonic and isostatic implications. Earth and Planetary Science Letters 297, 71–83.

Aitken, A.R.A., Salmon, M.L. and Kennett, B.L.N. (2013). Australia's Moho: A test of the usefulness of gravity modelling for determination of Moho depth. Tectonophysics, Vol. 609, pp. 468-479.

Aitken, A.R.A., Betts, P.G., Weinberg, R.F. and Gray, D. (2009). Constrained potential field modeling of the crustal architecture of the Musgrave Province in central Australia: evidence for lithospheric strengthening due to crust-mantle boundary uplift. Journal of Geophysical Research B: Solid Earth 114.

Ajayi, C.O. and Ajakaiye, D.E. (1981). The origin and peculiarities of the Nigerian Benue Trough: another look from recent gravity data obtained from the Middle Benue. *In:* R. Freund and Z. Garfunkel (eds.), the Dead Sea Rift. Tectonophysics, 80, pp. 285-303.

Ajayi, C.O. and Ajakaiye, D.E. (1986). Structures deduced from gravity data in the middle Benue Nigeria. Journal of African Earth Sciences, Vol. 5, No. 4, pp. 359-369.

Ajibade, A.C. And Wright, J.B. (1989). The Togo-Benin-Nigeria Shield: evidence of crustal aggregation in the Pan-African belt. Tectonophysics, Vol. 165, pp. 125-129.

Ajibade, A.C., Woakes, M. and Rahaman, M.A. (1989). Proterozoic crustal development in the Pan-African regime of Nigeria. In Kogbe, C. A. (Ed.), Geology of Nigeria. Rock View (Nigeria) Ltd., Jos. Pp. 57-69.

Akande, S.O., Horn, E.E. and Reutel, C. (1988). Mineralogy, fluid inclusion and genesis of the Arufu and Akwana Pb-Zn-F mineralisation, middle Benue Trough Nigeria. Journal of African Earth Sciences, Vol. 7, No. 1, pp. 167-180.

Akande, O., Zentelli, M. and Reynolds, P.H. (1989). Fluid inclusion and stable isotope studies of Pb-Zn-fluorite-barite mineralization in lower and middle Benue Trough, Nigeria. Mineral Deposita, Vol. 24, pp. 183-191.

Akpan, O., Nyblade, A., Okereke, C., Oden, M., Emry, E. and Julia, J. (2016). Crustal structure of Nigeria and southern Ghana, West Africa from P-wave receiver functions. Tectonophysics, http://dx.doi.org/10.1016/j.tecto.2016.02.005

Allen, P.A. and Allen, J.R. (2013). Basin Analysis: Principles and application to petroleum play assessment. Third Edition. Wiley-Blackwell, A John Wiley & Sons Ltd Publication, Oxford UK. 619p.

Anudu, G.K. (2017). Evaluation of the crustal structure of the middle Benue Trough, Nigeria, based on the analysis of potential field data. Ph.D. Thesis, University of Aberdeen, Aberdeen, Scotland United Kingdom (Unpublished). 391p.

Anudu, G.K., Stephenson, R.A., Ofoegbu, C.O. and Obrike, S.E. (2020). Basement morphology of the middle Benue Trough, Nigeria, revealed from analysis of high-resolution aeromagnetic data using grid-based operator methods. Journal of African Earth Sciences, Vol. 162, 103724.

Anudu, G.K., Stephenson, R.A. and Macdonald, D.I.M. (2014). Using high-resolution aeromagnetic data to recognise and map intra-sedimentary volcanic rocks and geological structures across the Cretaceous middle Benue Trough, Nigeria. Journal of African Earth Sciences, Vol. 99, pp. 625-636.

Anudu, G.K., Onuba, L.N., Onwuemesi, A.G. and Ikpokonte, A.E. (2012). Analysis of aeromagnetic over Wamba and its adjoining areas in north-central Nigeria. Earth Sciences Research Journal, Vol. 16, No. 1, pp. 25-33.

Avbovbo, A., Ayoola, E. and Osahon, G. (1986). Depositional and structural styles in Chad Basin of northeastern Nigeria. AAPG Bulletin, Vol. 70, pp. 1787-1798.

Badejoko, T.A. (1986). Triclinicity of K-feldspars and trace element content of Mesozoic granites of Central Nigeria. Chemical Geology, Vol. 54, pp. 43-51.

Balmino, G., Vales, N., Bonvalot, S. and Briais, A. (2012). Spherical harmonic modelling to ultra-high degree of Bouguer and isostatic anomalies. Journal of Geodesy, Vol. 86, pp. 499-520. http://dx.doi.org/10.1007/s00190-011-0533-4.

Benkhelil, J. (1986). Structure et evolution geodynamique due bassin intracontinental de la Benoue (Nigeria). These Sciences, Nice, 231p.

Benkhelil, J. (1989). The origin and evolution of the Cretaceous Benue Trough (Nigeria). Journal of African Earth Sciences, Vol. 6, pp. 251-282.

Benkhelil, J., Dainelli, P., Ponsard, J.F., Popoff, M. and Saugy, L. (1988). The Benue Trough: Wrench-fault related basin on the border of the Equatorial Atlantic. *In:* Manspeizer, W. (ed.), Triassic-Jurassic Rifting: Continental breakup and the origin of the Atlantic Ocean and passive margin. Part A, Developments in Geotectonics 22. Elsevier Science Publishers B. V., Amsterdam, the Netherlands. 998p.

Benkhelil, J., Guiraud, M., Ponsard, J.F. and Saugy, L. (1989). The Bornu-Benue Trough, the Niger Delta and its offshore: Tectono-sedimentary reconstruction during the Cretaceous and Tertiary from geophysical data and geology. *In:* Kogbe, C. A. (ed.), Geology of Nigeria (2nd revised edition). Rock View (Nigeria) Ltd., Jos. pp. 277-309.

Bermingham, P.M., Fairhead, J.D. and Stuart, G.W. (1983). Gravity study of the Central African Rift System: a model of continental disruption. 2: the Darfur domal uplift and associated Cainozoic volcanism. Tectonophysics, Vol. 94, pp. 205-222.

Billings, S. and Richards, D. (2000). Quality control of gridded aeromagnetic data. Exploration Geophysics, Vol. 31, No.4, pp. 611-616.

Blakely, R.J., Sherrod, B.L., Weaver, C.S., Wells, R.E. and Rohay, A.C. (2014). The Wallula fault and tectonic framework of south-central Washington, as interpreted from magnetic and gravity anomalies. Tectonophysics, Vol. 624-625, pp. 32-45.

Bocin, A., Stephenson, R., Matenco, L. and Mocanu, V. (2013). Gravity and magnetic modelling in the Vrancea Zone, south-easternCarpathians: Redefinition of the edge of the East European Cratonbeneath the south-eastern Carpathians. Journal of Geodynamics, Vol. 71, pp. 52-64.

Bonvalot, S., Balmino, G., Briais, A., Kuhn, M., Peyrefitte, A., Vales, Biancale, R., Gabalda, G., Moreaux, G., Reinquin, F. and Sarraillh, M. 2012. *In:* World Gravity Map, Vol. 1. Bureau Gravimetrique International (BGI) e Commission for the Geological Map of the World (CGMW), Centre National d'Etudes Spatiales (CNES) e Institut de Reserche pour le Development (IRD), Paris, p. 50,000,000.

Bowden, P. and Kinnaird, J.A. (1984). Geology and mineralisation of the Nigerian anorogenic ring complexes. Beith Geologisches Jahrbuch, Vol. B56, pp. 197-299.

Bowden, P., Black, R., Martin, R.F., Ike, E.C., Kinnaird, J.A. and Batchelor, R.A. (1987). Niger-Nigeria alkaline ring complexes: a classic example of African Phenerozoic anorogenic mid-plate magmatism. *In:* Fitton, J. G. and Upton, B. G. J. (eds.) Alkaline Igneous Rocks. Geological Society Special Publication, No. 30, pp. 357-379.

Braitenberg, C. (2012). LithoFLEX Version 2.0. Department of Earth Sciences, University Trieste, Trieste Italy.

Braitenberg, C., Wienecke, S., Ebbing, J., Born, W., Redfield, T. and Mariani, P. (2008). LithoFLEX Tutorial user's manual. LithoFLEX Group, Trieste, Italy. [Available at http://www.lithoflex.org/lithoflex/home/basics/Lithoflex_tutorial.pdf.]

Braitenberg, C., Wienecke, S. and Wang, Y. (2006). Basement structures from satellite-derived gravity field: South China Sea ridge. Journal of Geophysical Research, Vol. 111, B05407, 15p.

Braitenberg, C., Zadro, M., Fang, J., Wang, Y. and Hsu, H. T. (2000a). Gravity inversion in Qinghai-Tibet-Plateau. Phys. Chem. Earth, Part A, 25(4), pp. 381-386.

Braitenberg, C., Zadro, M., Fang, J., Wang, Y. and Hsu, H.T. (2000b). The gravity and isostatic Moho undulations in Qinghai-Tibet-Plateau. J. Geod., 30 (5), pp. 489-505.

Burke, K.C. and Dewey, J.F. (1974). Two plates in Africa during the Cretaceous? Nature, London, Vol. 249, pp. 313-316.

Burke, K.C. and Whiteman, A.J. (1973). Uplift, rifting and the break-up of Africa. *In:* Tarling, D. H. and Runcorn, S. K. (eds.), Implications on continental drift to Earth Sciences, pp. 735-755.

Cloetingh, S., Ziegler, P.A., Beekman, F., Burov, E.B., Garcia-Castellanos, D. and Matenco, L. (2015). Tectonic models for the evolution of sedimentary basins. *In:* Schubert, G. (ed.) Treatise on Geophysics, (2nd edition). Elsevier B.V. pp. 513-592.

Cratchely, C.R. and Jones, G.P. (1965). An interpretation geology and gravity anomalies of the Benue valley Nigeria. Oversea Geological Survey London, Geophysics. Paper No. 1.

Curto, J.B., Vidotti, R.M., Blakely, R.J. and Fuck, R.A. (2015). Crustal framework of the northwest Parana Basin, Brazil: insights from joint modelling of magnetic and gravity data. Tectonophysics, Vol. 655, pp. 58-72.

Dada, S.S. (1999). Geochemistry and petrogenesis of the reworked Archaean gneiss complex of north-central Nigeria: major and trace element studies on Kaduna amphibolite and migmatitic gneisses. Global Journal of Pure and Applied Sciences, Vol. 5, pp. 535-543.

Damiani, T.M., Jordan, T.A., Ferraccioli, F., Young, D.A. and Blankenship, D.D. (2014). Variable crustal thickness beneath Thwaites Glacier revealed from airborne gravimetry, possible implications for geothermal heat flux in West Antarctica. Earth and Planetary Science Letters, Vol. 407, pp. 109-122.

Dobrin, M.B. and Savit, C.H. (1988). Introduction to Geophysical Prospecting, 4th edition, McGraw-Hill, New York. 867p.

Ebbing, J., Braitenberg, C. and Wienecke, S. (2007). Insights into the lithosphere structure and tectonic setting of the Barents Sea region from isostatic considerations. Geophys. J. Int. Vol. 171, pp. 1390-1403.

Fairhead, J.D. (2015). Advances in gravity and magnetic processing and interpretation. E-book. EAGE Publications, The Netherlands. 220p.

Fairhead, J.D. and Binks, R.M. (1991). Differential opening of the Central and South Atlantic Oceans and the opening of the West African rift system. Tectonophysics, Vol. 187, pp. 191-203.

Fairhead, J.D. and Green, C.M. (1989). Controls on rifting in Africa and the regional tectonic model for the Nigeria and East Niger rift basins. Journal of African Earth Sciences, Vol. 8, Nos. 2/3/4, pp. 231-249.

Fairhead, J.D., Green, C.M. and Guiraud, R. (2013). The role that plate tectonics, inferred stress changes and stratigraphic unconformities have on the evolution of the West and Central African Rift System and the Atlantic continental margins. Tectonophysics, Vol. 594, pp. 118-127.

Fairhead, J.D. and Okereke, C.S. (1987). A regional gravity study of the West African rift system in Nigeria and Cameroon and its tectonic interpretation. *In:* I. B. Ramberg, E. E. Milanovsky and G. Qvale (eds.), Continental Rifts – Principal and Regional Characteristics. Tectonophysics, Vol. 143, pp. 141-159.

Fairhead, J.D. and Okereke, C.S. (1988). Depths to major density contrasts beneath the West African rift system in Nigeria and Cameroon based on the spectral analysis of gravity data. Journal of African Earth Sciences, Vol. 7, No. 5/6, pp. 769-777.

Fairhead, J.D. and Okereke, C.S. (1990). Crustal thinning and extension beneath the Benue Trough based on gravity studies. Journal of African Earth Sciences, Vol. 11, No. 3/4, pp. 329-335.

Fichler, C., Odinsen, T., Rueslatten, H., Olesen, O., Vindstad, J.E. And Wienecke, S. (2011). Crustal inhomogeneities in the Northern North Sea from potential field modelling: Inherited structure and serpentinities? Tectonophysics, Vol. 510, pp. 172-185.

Gallacher, R.J. and Bastow, I.D. (2012). The development of magmatism along the Cameroon Volcanic Line: evidence from teleseismic receiver functions. Tectonics, Vol. 31, TC3018.

Guiraud, M. (1990). Tectono-sedimentary framework of the early Cretaceous continental Bima Formation (Upper Benue Trough, NE Nigeria). Journal of African Earth Sciences, Vol. 10, pp. 341-353.

Guiraud, R. and Maurin, J.C. (1991). Le rifting enAfrique au Cretaceinferieur: synthese structural, miseen evidence de deux phases dans la genese des basins, relations avec les ouverturesoceaniquesperi-africaines. Bull. Soc. Geol. Fr., 162, pp. 811-823.

Guiraud, R. and Maurin, J.C. (1992). Early Cretaceous rifts of Western and Central African. *In:* P. A., Ziegler (ed.), Geodynamics of rifting, Vol. II. Case history studies on rifts: North and South America and Africa. Tectonophysics, Vol. 213, pp. 153-168.

Guiraud, R. and Maurin, J.C. (1993). Cretaceous rifting and basin inversion in Central Africa. *In:* Thorweihe, U., and Schandelmeier, H. (Eds.), Geoscientific Research in northeast Africa: Rotterdam (A. A. Balkema), pp. 203-206.

Guiraud, M., Ajakaiye, D.E. and Ugodulunwa, F.X.O. (1989). Characterisation of Late Cretaceous NE-SW sinistral wrench faults in the upper Benue Trough (Nigeria) using microtectonic and aeromagnetic data. Journal of African Earth Sciences, Vol. 9, No. 1, pp. 9-21.

Guiraud, R., Bosworth, W., Thierry, J. and Delplanque, A. (2005). Phanerozoic geological evolution of Northern and Central Africa: An overview. Journal of African Earth Sciences, Vol. 43, pp. 83-143.

Hinze, W.J., Von Frese, R.R.B. and Saad, A.H. (2013). Gravity and Magnetic Exploration. Principles, Practices and Applications. Cambridge University Press, New York. 512p.

Jacoby, W. and Smilde, P.L. (2009). Gravity Interpretation: Fundamentals and application of gravity inversion and geological interpretation. Springer-Verlag Berlin Heidelberg. 387p.

Jarvis, A., Reuter, H.I., Nelson, A. and Guevara, E. (2008). Hole-filled SRTM for the globe Version 4, available from the CGIAR-CSI SRTM 90m Database (http://srtm.csi.cgiar.org).

Jassen, M.E., Stephenson, R.A. and Cloetingh, S. (1995). Temporal and spatial correlations between changes in plate motions and the evolution of rifted basins in Africa. Geological Society of America (GSA) Bulletin, Vol. 107, No. 11, pp. 1317-1332.

Jordan, T.A., Ferraccioli, F., Ross, N., Corr, H.F.J., Leat, P.T., Bingham, R.G., Rippin, D.M., Brocq, A.L. and Siegert, M.J. (2013). Inland extent of the Weddell Sea Rift imaged by new aerogeophysical data. Tectonophysics Vol. 585, pp. 137-160.

Kusznir, N.J., Roberts, A.M. and Alvey, A.D. (2018). Crustal structure of the conjugate Equatorial Atlantic Margins derived by gravity anomaly inversion. *In:* McClay, K. R. and Hammerstein, J. A. (eds.), Passive Margins: Tectonics, Sedimentation and Magmatism. Geological Society, London, Special Publications, Vol. 476, pp. 83-107.

Long, L.T. and Kaufmann, R.D. (2013). Acquisition and analysis of terrestrial gravity data. Cambridge University Press, New York USA. 171p.

Maguire, P.K.H., Keller, G.R., Klemperer, S.L., Mackenzie, G.D., Keranen, K., Harder, S., O'reilly, B.O., Thybo, H., Asfaw, L., Khan, M.A. and Amha, M. (2006). Crustal structure of the northern Main Ethiopian Rift from the EAGLE controlled-source survey; a snapshot of incipient lithospheric break-up. *In:* Yirgu, G., Ebinger, C. J. and Maguire, P. K. H. (eds.), The Afar volcanic province within the East African Rift System. Geological Society, London, Special Publications, Vol. 259, pp. 269-291.

Maluski, H., Coulon, C., Popoff, M. and Baudin, P. 1995. $^{40}Ar/^{39}Ar$ chronology, petrology and geodynamic setting of Mesozoic to early Cenozoic magmatism from the Benue Trough, Nigeria. Journal of the Geological Society, London, Vol. 152, pp. 311-326.

Maurin, J.C., Benkhelil, J. and Robineau, B. (1986). Fault rocks of the Kaltungo lineament, N.E. Nigeria and their relationship with Benue Trough tectonics. Journal of Geological Society London, Vol. 143, pp. 587-599.

Mazur, S., Green, C., Stewart, M.G., Whittaker, J.M., Williams, S. and Bouatmani, R. (2012). Displacement along the Red River Fault constrained by extension estimates and plate reconstructions. Tectonics, Vol. 31, TC5008, 22p.

McCurry, P. (1989). A general review of the geology of the Precambrian to Lower Palaeozoic rocks of northern Nigeria. In Kogbe, C. A. (Ed.), Geology of Nigeria. Rock View (Nigeria) Ltd., Jos. Pp. 13-37.

McKenzie, D. (1978). Some remarks on the development of sedimentary basins. Earth Planet. Sci. Lett., Vol. 40, pp. 25-32.

Mohamed, A.Y., Ashcroft, W.A. and Whiteman, A.J. (2001). Structural development and crustal stretching in the Muglad Basin, southern Sudan. Journal of African Earth Sciences, Vol. 32, No. 2, pp. 179-191.

Nabighian, M.N., Ander, M.E., Grauch, V.J.S., Hansen, R.O., LaFehr, T.R., Li, Y., Pearson, W.C., Peirce, J.W., Philips, J.D. and Ruder, M.E. (2005). Historical development of the gravity method in exploration. 75th Anniversary Society of Exploration Geophysicists. Geophysics, Vol. 70, No. 6, pp. 63ND-89ND.

NGSA (Nigerian Geological Survey Agency), (2009). Geological and mineral resources map of Nigeria. Authority of Federal Republic of Nigeria.

Nwajide, C.S. (2013). Geology of Nigeria's Sedimentary Basins. CSS Press (A division of CSS Bookshops Limited) Lagos Nigeria. 565p.

Oakey, G.N. and Stephenson, R. (2008). Crustal structure of the Innuitian region of Arctic Canada and Greenland from gravity modelling: implications for the Palaeogene Eurekan orogen. Geophysical Journal International, Vol. 173, pp. 1039-1063.

Obaje, N.G. (2009). Geology and mineral resources of Nigeria. Springer Dordrecht. 221p.

Obaje, N.G. and Hamza, H. (2000). Liquid hydrocarbon source-rock potential of mid-Cretaceous coals and coal measures in the middle Benue Trough of Nigeria. Int. Jour. Earth Sci., Vol. 89, pp. 130-139.

Obiora, S.C. (2002). Evaluation of the effects of igneous bodies on the sedimentary fills of the lower Benue Rift and vice versa. PhD Thesis, University of Nigeria, Nsukka (Unpublished). 241p.

Offodile, M.E. (1976). The geology of middle Benue Trough, Nigeria. Special Volume Palaeontological Institution of University of Uppsala, Vol. 4, pp. 1-66.

Offodile, M.E. (1980). A mineral survey of the Cretaceous of the Benue Valley, Nigeria. Cretaceous Research, Vol. 1, pp. 101-124.

Offodile, M.E. (1989). A review of the geology of the Cretaceous of the Benue Valley. *In:* Kogbe, C. A. (ed.), Geology of Nigeria (2nd revised edition). Rock View Nigeria Ltd, Jos. 538p.

Offodile, M.E. and Reyment, R.A. (1977). Stratigraphy of the Keana-Awe area of the middle Benue region of Nigeria. Bulletin of Geological Institutions University of Uppsala (N.S), Vol. 7, pp. 37-66.

Okereke, C.S. (1988). Contrasting modes of rifting: The Benue Trough and Cameroon Volcanic Line, West Africa. Tectonics, Vol. 7, No. 4, pp. 775-784.

Olade, M.A. (1975). Evolution of Nigeria's Benue Trough (Aulacogen): a tectonic model. Geol. Mag., Vol. 112, No. 6, pp. 575-583.

Oldenburg, D.W. (1974). The inversion and interpretation of gravity anomalies. Geophysics, Vol. 39, pp. 526-583.

Osazuwa, I.B., Ajakaiye, D.E. and Verheijen, P.J.T. (1981). Analysis of the structure of part of the Benue Rift Valley on the basis of new geophysical data. Earth Evol. Sci., Vol. 1, pp. 126-136.

Parker, R.L. (1972). The rapid calculation of potential anomalies. Geophys. J. R. Astron. Soc., Vol. 31, pp. 447-455.

Rahaman, M.A. (1989). Review of the basement geology of south-western Nigeria. In Kogbe, C. A. (Ed.), Geology of Nigeria. Rock View (Nigeria) Ltd., Jos. Pp. 39-58.

Rahaman, M.A., Van Breemen, O., Bowden, P. and Bennett, J.N. (1984). Age migration of anorogenic ring-complexes in northern Nigeria. Journal of Geology, Vol. 93, No. 3, pp. 173-184.

Sheriff, R.E. (2002). Encyclopedic Dictionary of Applied Geophysics, 4th edition. 13 Geophysical Reference Series. Society of Exploration Geophysicists, Tulsa USA, 429p.

Steffen, R., Strykowski, G. and Lund, B. (2017). High-resolution Moho model for Greenland from EIGEN-6C4 gravity data. Tectonophysics, Vol. 706-707, pp. 206-220.

Steffen, R., Steffen, H. and Jentzsch, G. (2011). A three-dimensional Moho depth model for the Tien Shan from EGM2008 gravity data. Tectonics, Vol. 30, TC5019, 15p.

Stephenson, R.A., Coflin, K.C., Lane, L.S. and Dietrich, J.R. (1994). Crustal structure and tectonics of the southeastern Beaufort Sea continental margin. Tectonics, Vol. 13, No. 2, pp. 389-400.

Stephenson, R., Piepjohn, K., Schiffer, C., Von Gosen, W., Oakey, G.N. and Anudu, G. (2017). Integrated crustal-geological cross-section of Ellesmere Island. *In:* Pease, V. and Coakley, B. (eds.) Circum-Arctic Lithosphere Evolution. Geological Society, London, Special Publications, Vol. 460, pp. 7-17. https://doi.org/10.1144/SP460.12.

Stuart, G.W., Fairhead, J.D., Dorbath, L. and Dorbath, C. (1985). A seismic refraction study of the crustal structure associated with the Adamawa Plateau and Garoua Rift, Cameroon, West Africa. Geophysical Journal of Royal Astronomical Society, Vol. 81, No. 1, pp. 1-12.

Su, D., White, N. and McKenzie, D. (1989). Extension and subsidence of the Pearl River Mouth Basin, northern South China Sea. Basin Research, Vol. 2, pp. 205-222.

Suleiman, A.A., Magee, C., Jackson, A.-L. and Fraser, A.J. (2017). Igneous activity in the Bornu Basin, onshore NE Nigeria; implications for opening of the South Atlantic. Journal of the Geological Society, Vol. 174, pp. 667-678.

Telford, W.M., Geldart, L.P. and Sheriff, R.E. (1998). Applied Geophysics, 2nd edition, Cambridge University Press, USA.770p.

Tiberi, C., Ebinger, C., Ballu, V., Stuart, G. and Oluma, B. (2005). Inverse models of gravity data from the Red Sea-Aden-East African rifts triple junction zone. Geophysical Journal International, Vol. 163, pp. 775-787.

Tokam, A.P.K., Tabod, C.T., Nyblade, A.A., Julià, J., Wiens, D.A. and Pasyanos, M.E. (2010). Structure of the crust beneath Cameroon, West Africa, from the joint inversion of Rayleigh wave group velocities and receiver functions. Geophysical Journal International, Vol. 183, No. 2, pp. 1061-1076.

Umeji, A.C. (1985). Geology and petrochemistry of some of the volcanic and subvolcanic rocks in lower Benue Trough. Journal of Mining and Geology, Vol. 22, Nos. 1-2, p. 199-204.

Umeji, A.C. (2000). Evolution of the Abakaliki and the Anambra basins, southeastern nigeria. A report submitted to Shell Petrolum Development Company Nigeria Ltd. 155p.

Van der Meijde, M., Julia, J. and Assumpcao, M. (2013). Gravity derived Moho for South America. Tectonophysics, Vol. 609, Pp. 456-467.

Whiteman, A.J. (1982). Nigeria: its petroleum geology resources and potential. Graham and Trotman, London UK. Vol. 1, 176p; Vol. 2, 238p.

Wilson, M. and Guiraud, R. (1992). Magmatism and rifting in Western and Central Africa, from Late Jurassic to Recent times. Tectonophysics, 213, pp. 203-225.

Woakes, M., Rahaman, M.A. and Ajibade, A.C. (1987). Some metallogenetic features of the Nigerian basement. Journal of African Earth Science, Vol. 6, pp. 54-64.

Wright, J.B. (1976). Origins of the Benue Trough – a critical review *In:* C. A. Kogbe (ed.) Geology of Nigeria. Elizabethan Publication Co., Lagos, pp. 313 -318.

Wright, J.B. (1981). Review of Origins Evolution of the Benue Trough in Nigeria. Earth Evolution Science, Vol. 2, pp. 98 -103.

Wright, J.B., Hastings, D.A., Jones, W.B. and Williams, H.R. (1985). Geology and mineral resources of West Africa. George Allen & Unwin (Publishers) Ltd, London UK. 190p.

Ziegler, P.A. and Cloetingh, S. (2004). Dynamic processes controlling evolution of rifted basins. Earth Science Reviews, Vol. 64, pp 1-50.